EXPERIMENTAL OPTIMIZATION OF ABS CONTENT IN PC FOR ENHANCED SYNERGISM EFFECT OF PC/ABS BLEND IN CFRP COMPOSITES WITH ENHANCED FRACTURE TOUGHNESS

PROJECT REPORT

Submitted by

KASTHOORI M S

TKM20MECI05

to

the APJ Abdul Kalam Technological University

in partial fulfillment of the requirements for the award of Degree

of

Master of Technology

In

Computer Integrated Manufacturing

DEPARTMENT OF MECHANICAL ENGINEERING

T.K.M. College of Engineering

Kollam 691005, Kerala

SEPTEMBER, 2022

DECLARATION

I Kasthoori M S, hereby declare that the project report entitled “Experimental optimization of ABS content in PC for enhanced synergism effect of PC/ABS blend in CFRP composites with enhanced fracture toughness ", submitted for partial fulfillment of the requirements for the award of degree of Master of Technology of the APJ Abdul Kalam Technological University, Kerala is a bonafide work done by me under supervision of Dr. K.E. Reby Roy, Professor, Department of Mechanical Engineering, TKMCE Kollam. This submission represents my ideas in my own words and where ideas or words of others have been included. I have adequately and accurately cited and referenced the original sources. I also declare that I have adhered to ethics of academic honesty and integrity and have not misrepresented or fabricated any data or idea or fact or source in my submission. I understand that any violation of the above will be a cause for disciplinary action by the institute and/or the University and can also evoke penal action from the sources which have thus not been properly cited or from whom proper permission has not been obtained. This report has not been previously formed the basis for the award of any degree, diploma or similar title of any other University.

Kollam

12/09/2022 KASTHOORI M S

DEPARTMENT OF MECHANICAL ENGINEERING

TKM COLLEGE OF ENGINEERING, KOLLAM

CERTIFICATE

This is to certify that the project report entitled **'EXPERIMENTAL OPTIMIZATION OF ABS CONTENT IN PC FOR ENHANCED SYNERGISM EFFECT OF PC/ABS BLEND IN CFRP COMPOSITES WITH ENHANCED FRACTURE TOUGHNESS'** submitted by **KASTHOORI M S, TKM20MECI05** to the APJ Abdul Kalam Technological University in partial fulfillment of the requirements for the award of the Degree of Master of Technology in Computer Integrated Manufacturing, Department of Mechanical Engineering is a bonafide record of the project work carried out by her under our guidance and supervision. This report in any form has not been submitted to any other University or institute for any purpose.

Supervisor: **Dr. K.E. Reby Roy**

Professor

Dept. of Mechanical Engineering

TKM College of engineering, Kollam

P G Coordinator: **Prof. Kannan S.**

Assistant Professor

Dept. of Mechanical Engineering

TKM College of engineering, Kollam

Dr. Dileep P.N.

Head of the department

Dept. of Mechanical Engineering

TKM College of engineering, Kollam

ACKNOWLEDGEMENT

I take this opportunity to express my deep sense of gratitude and sincere thanks to all who helped me to complete the project successfully.

I am greatly thankful to **Dr. T.A. Shahul Hameed**, Principal, TKM College of Engineering, and **Dr. Dileep P.N.**, Head of Mechanical Engineering Department for their support and cooperation.

I am deeply indebted to my guide **Dr. K.E. Reby Roy**, Professor, Department of Mechanical Engineering for his excellent guidance, positive criticism, and valuable comments.

My heartfelt gratitude to **Prof. Kannan S.**, PG coordinator, Department of Mechanical Engineering, and **Prof. Faizal N.S.**, Assistant Professor, Department of Mechanical Engineering for their valuable suggestions and guidance in the preparation of the project presentation and report.

I am highly thankful to **Mr. Aravind J.**, Research Scholar (Ph.D.), Department of Mechanical Engineering for his great support and guidance in the successful completion of this project.

I am thankful to Cornell Center for Materials Research (CCMR), Cornell University, USA, and FAN Services, Maharashtra, India for their timely help and support to complete my project.

I also express my thanks to the teaching and non-teaching staff of T.K.M. College of Engineering who have supported us in the successful completion of our project.

I will be failing in duty if I do not acknowledge with thanks to the authors of the references and other literature referred to this project.

Finally, I thank my parents, friends, and near and dear ones who directly and indirectly contributed to the successful completion of my project.

Kollam

12/09/2022 **KASTHOORI M S**

ABSTRACT

Thermoplastic modification of Bisphenol A diglycidyl ether (DGEBA epoxy resin) is commonly performed for achieving enhanced fracture toughness and increased interlaminar strength in carbon fiber reinforced polymer (CFRP) composites. The thermoplastic content required for modification of epoxy usually lies in the range of 15-20 weight percentage (wt.%), making it difficult to be used with hand lay-up and resin infusion techniques. In this study, the synergism effect achieved with the presence of polycarbonate (PC) and acrylonitrile butadiene styrene (ABS) blend modified DGEBA is reported for lower wt% of thermoplastic content (1.5wt%). The concentration of ABS in PC is optimized for a positive synergism effect in toughening of the epoxy matrix via melt-mixing and it is critically analyzed using the FTIR, DSC, and TGA. Subsequently, interlaminar fracture toughness and strain energy release rate of unmodified and PC/ABS (90/10) blend modified CFRP are studied using mode I, II, and Mix-mode test and confirms that the blend 90/10 successful improves the interlaminar strength (ILSS) by 84.2%, 72.1%, and 89.4% respectively and enhances the strain energy release rate (SERR) by 218.1%, 103.1%, and 195.8% respectively and a 17.3% increase in elongation at break. It is interesting to find nano web-like morphology in PC/ABS blend modified CFRP resulting in enhanced mechanical, reduced brittle nature, and increased thermal stability. The present study confirms using a 90/10 blend at 1.5wt% to modify CFRP composites with excellent interlaminar strength and reduced brittle nature, supporting future works in developing structural elements, passenger compartments, and body panels in the automobile industry.

Keywords: *Thermoplastic modification, melt-mixing, epoxy toughening, ILSS, SERR, automobile applications.*

CONTENTS

LIST OF TABLES

LIST OF FIGURES

ABBREVIATIONS

ABS	Poly(acrylonitrile butadiene styrene)
CF	Carbon fiber
CFRP	Carbon fiber reinforced polymer
CT	Cryogenic temperature
CTE	Coefficient of thermal expansion
DGEBA	Diglycidyl ether of bisphenol A
DSC	Differential Scanning Calorimetry
EP	Epoxy
FTIR	Fourier transform infrared
IPN	Interpenetrating polymer networks
PBT	Poly butylene terephthalate
PC	Polycarbonate
PE	Polyethylene
PEI	Polyetherimide
PET	Polyethylene Terephthalate
PP	Polypropylene
PS	Polystyrene
RT	Room temperature
SEM	Scanning electron microscope
TGA	Thermogravimetric analysis
VARTM	Vacuum-assisted resin transfer molding
ILSS	Interlaminar shear strength
SERR	Strain energy release rate

NOTATION

A	Cross-sectional area, m^2
a	Delamination length, mm
b	Specimen width, mm
d	Specimen thickness, mm
L	Support span, mm
P	Ultimate Tensile Load, N

CHAPTER 1
INTRODUCTION

1.1 CARBON FIBER (CF)

Carbon atoms are joined in a long chain via chemical bonds to create carbon fibre. Typically, carbon fibres have a diameter of 5 to 10 micrometres. a material that is both incredibly strong and light. High stiffness, good tensile strength, low weight, high chemical resistance, high-temperature tolerance, and minimal thermal expansion are some of the most notable characteristics of carbon fibres. Carbon fibre reinforced composites are five times stronger than steel, twice as rigid, and around two-thirds the weight when compared to steel. The carbon fibre strands are so tiny that they are even thinner than a human hair. The carbon fibre strands can be twisted together to create yarn and they can be woven together to create a garment that will be very light in weight. Carbon fibre can be reinforced in a variety of ways, depending on the application, including as a thin yarn or tow, a fabric that can be woven in a particular pattern, like a plain weave or twill weave, or as cloth.

In addition to the advantages listed above, they are rather pricey when compared to other fibres of a similar nature, such as glass or plastic. Carbon atoms must be bound in a specific way to create crystals and must be oriented so that the long axis of the fibre is parallel to the crystals formed for the creation of carbon fibres to be effective. The crystal alignment has already shown a good strength-to-volume ratio. The atomic structures of carbon fibre and graphite are comparable. Carbon atoms are arranged in sheets in a regular hexagonal pattern (graphene sheets). But how these sheets interlock makes a difference. When carbon fibres are used in a composite with other materials, their strength is shown. Typically, resins are used to reinforce

carbon fibres, and when they are cured, they produce a superior material with greater qualities than the neat resin alone.

1.1.1 Structure and properties of CF

A continuous tow coiled onto a reel is a common kind of carbon fibre supply. The tow is a mass made up of numerous thousands of small carbon filaments that are bound together and shielded by an organic size, such as polyethylene oxide (PEO) or polyvinyl alcohol (PVA). For use, the tow can easily be unwound from the reel. Each of the tow's carbon filaments is a continuous cylinder with a 5–10 micrometer diameter that is virtually entirely made of carbon. Diameters of the earliest generation ranged from 16 to 22 micrometers (for example, T300, HTA, and AS4). The diameter of later fibres, like IM6 or IM600, is roughly 5 micrometers. While graphite and carbon fibre both have sheets of carbon atoms arranged in a regular hexagonal pattern (graphene sheets), the way these sheets interlock in carbon fibre is different. In the crystalline substance known as graphite, the sheets are regularly arranged parallel to one another. Graphite's soft and brittle qualities are caused by Van der Waals forces, which are relatively weak intermolecular forces between the sheets.

Carbon fibre can be turbostratic, graphitic, or have a hybrid structure with both graphitic and turbostratic components depending on the precursor used to manufacture the fibre. The carbon atom sheets that make up turbostratic carbon fibre are randomly folded or crumpled. Turbostratic carbon fibres are made of polyacrylonitrile (PAN), whereas graphitic carbon fibres are made of mesophase pitch and undergo heat treatment at temperatures above 2200 °C. While heat-treated mesophase-pitch-derived carbon fibres have high Young's modulus (i.e., high stiffness or resistance to extension under load) and high thermal conductivity, turbostratic carbon fibres typically have high ultimate tensile strength.

1.1.2 Patterns of Carbon Fibers

A weaving loom is used to create fabrics from carbon fibre spools. The most popular weaves are harness satin, twill, and plain weave.

(i) Plain weave CF

Carbon fibre cloth with a plain weave, often known as a 1x1 weave, has a checkerboard-like symmetry as shown in figure 1.1. The tows have closely intertwined, extremely stable fibres because of the over/under weaving method. The ability of a material to hold onto its fibre orientation and weave angle is referred to as fabric stability. Because of its high fabric stability and lack of flexibility, plain weave carbon fibre cloth is not ideal for complex curves. It is simpler to handle without causing fabric distortions, though. As a result, it is effective for two-dimensional curves, tubes, and flat sheets. The curvature of a single fibre in a weave is known as crimp, and the tight interlacing in the tows of plain weave carbon fibre fabric gives it a harsh crimp. This severe crimping can produce stress points that, over time, lead to weak spots.

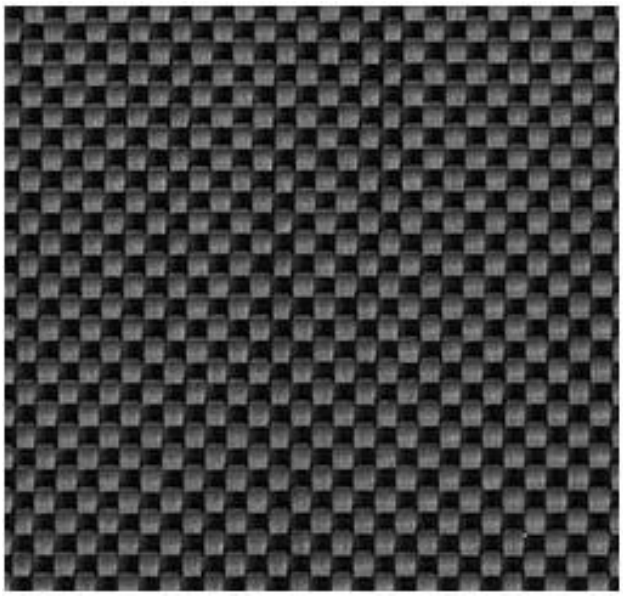

Figure 1.1 Plain weave CF

(ii) Twill weave CF

The most well-known variety of carbon fibre cloth is the twill weave, which has a 2x2 or 4x4 pattern as shown in figure 1.2. Each tow runs over two tows and then under two tows in a 2x2 weave. Therefore, it makes sense that each tow in a 4x4 weave crosses over four other tows before going below another four. This weaving creates a distinct diagonal pattern by going over and under. In a twill weave, the spacing between the two interlaces is greater than in a plain weave. As a result, there are fewer crimps and hence fewer opportunities for stress points to form.

Figure 1.2 Twill weave CF

(iii) Harness satin weave CF

Since ancient times, satin weaves have been employed to give silk fabric its lovely drape while still making the fabric smooth and seamless. Satin weaves translate to an ability to easily form around intricate curves when utilized for carbon fibre composites. This demonstrates that satin weaves are less stable than other weaves. Figure 1.3 shows the schematic structure of Satin weave carbon fiber.

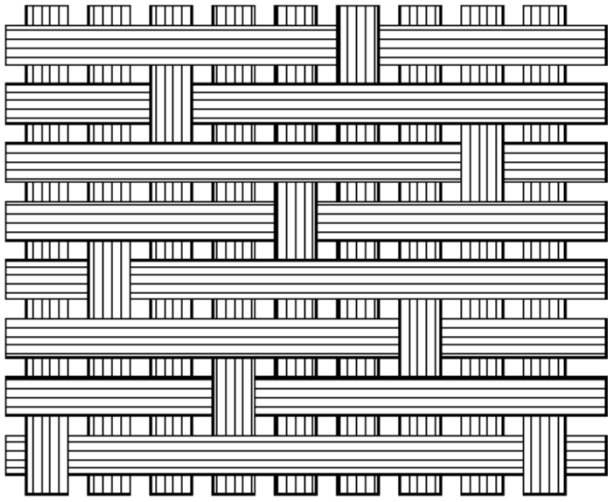

Figure 1.3 Harness satin weave CF

(iv) Unidirectional CF

These fabric patterns are non-woven and have fibres that are all oriented in one parallel direction. There won't be any spaces between the fibres in this design as shown in figure 1.4. When compared to other patterns, this pattern's main benefits include its extremely low weight and ability to offer maximal strength in the direction in which the fibres are laid (isotropic strength). Concerning the drawbacks, they have a poor aesthetic appearance for completed product parts and cannot be used for applications that call for anisotropic strength attributes.

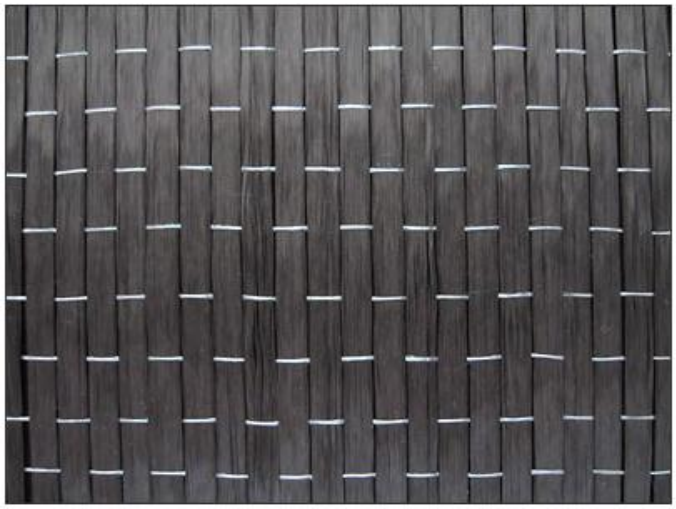

Figure 1.4 Unidirectional CF

1.1.3 Benefits of Carbon Fiber

- High stiffness
- High chemical resistance
- Excellent tensile strength
- Extremely temperature tolerance
- High wear resistance
- High corrosion resistance
- Great flexibility
- Low thermal expansion
- Low weight-to-strength ratio
- Good conductor of electricity

1.1.4 Applications of Carbon Fiber

- Most notably, carbon fibre is used to reinforce composite materials.
- The direct applications of carbon fibre filament yarns in textiles include prepregging, filament winding, pultrusion, weaving, braiding, etc.
- Carbon fibers are used for fabrication of carbon-fiber microelectrodes

1.2 EPOXY RESINS

A reactive prepolymer and polymer containing epoxide groups are referred to as epoxy resin. In the presence of catalysts, these resins either react with one another or with several co-reactants such as amines, phenols, thiols, etc.

Epoxy resin is used in the industry for a wide range of reasons. Compared to other forms of resin, it has higher mechanical qualities and greater heat and chemical resistance. As a result, it is only used to create components for aircraft. Polyepoxides is another name for epoxy resin.

1.2.1 Properties of Epoxy Resins

- Excellent stability
- High mechanical properties
- Flexibility and diversity in designing
- Good adhesive performance
- Good chemical and physical resistance when used as a material coating

1.2.2 Types of Epoxy Resins

There are two main kinds of epoxy resin: glycidyl and non-glycidyl. The subclasses of glycidyl resins are glycidyl-ether, glycidyl-ester, and glycidyl-amine. It will either be aliphatic or cyclo-aliphatic for the non-glycidyl type. The most popular are glycidyl-ether epoxies, especially those made of bisphenol and novolac.

(i) Bisphenol Epoxy Resins

One type of commercial epoxy resin that is frequently used is bisphenol-A diglycidyl ether (DGEBA). It is made when epichlorohydrin and bisphenol-A come into contact while a basic catalyst is present. The kind of epoxy resin with the least molecular weight is this one.

(ii) Aliphatic Epoxy Resins

These forms of epoxy resins are created either through a reaction with epichlorohydrin or double bond epoxidation, which uses cycloaliphatic epoxides and epoxidized vegetable oils (glycidyl ethers and esters).

(iii) Novolac Epoxy Resins

These kinds of resins are created when phenol and methanol come into contact and react (formaldehyde). Epoxyphenol novolac (EPN) or epoxycresol novolac are two examples of novolacs that are produced when epichlorohydrin and novolacs react (ECN). Solvents or volatile chemical substances are not present in these epoxies.

(iv) Halogenated Epoxy Resins

For these epoxy resins' unique qualities, additives are used. This entails the use of brominated and fluorinated cultivars in combination. For applications requiring flame resistance and electrical use, brominated bisphenol A is the material of choice. Due to the high related costs and low T_g, however, the commercial manufacturing and usage of such resins are constrained.

1.2.3 Advantages of Epoxy Resins

- The majority of materials can achieve strong bonding.
- Excellent chemical and other solvent resistance
- Promising mechanical and electrical insulating qualities
- Very little shrinkage while curing, which improves dimensional stability

1.2.4 Disadvantages of Epoxy Resins

- Limited pot life.
- Resins and hardeners must be handled carefully; otherwise, they may cause skin rashes and irritation.
- Cured material has little resistance to ultraviolet (Sunlight), which results in a color change of the cured substance when exposed to direct sunlight.

1.2.5 Applications of Epoxy Resins

- Metal coatings
- Use in electronic and electrical components

- Electrical insulators
- Fiber-reinforced plastic materials
- Structural adhesives

1.3 CARBON FIBER REINFORCED POLYMER (CFRP)

Carbon fiber reinforced polymers are composite materials that depend on carbon fiber to give strength and stiffness. In contrast, the polymer offers a cohesive matrix to safeguard and hold the fibers together and provides some toughness. Carbon fiber-reinforced plastic is referred to as CFRP. It is made up of a base or carrier substance called matrix and a second reinforcing component is known as carbon fiber incorporated into the matrix. As a matrix material, synthetic resin is typically employed. The type of carbon fibers deployed, the matrix, and the manufacturing methods all affect the cured composite's mechanical properties.

1.3.1 Carbon Fiber/Epoxy (CF/EP) Composite Modification using Thermoplastics

In this research, it is proposed to develop a carbon fiber-reinforced composite material. In essence, a composite material is a concoction of two or more materials with dissimilar physical and chemical properties. They can be mixed to produce a material that is specifically designed to carry out a certain task. Some of their attributes get better. For instance, it gets stronger, lighter, more electrically resistant, stronger, stiffer, etc. They are preferred over conventional materials because they enhance the underlying materials' qualities and can be used in a variety of contexts. According to extensive prior research, the ideal weight percentage for adding different thermoplastics for modification of DGEBA resin to increase impact resistance at both RT and CT is 1.5 wt%. This study chose a low wt% PC/ABS blend to toughen the epoxy matrix. In the current study, we seek to maximize the synergism with the chosen epoxy system to improve the mechanical and thermal properties of manufactured CFRP composites for aeronautical and structural applications at RT.

CHAPTER 2

LITERATURE REVIEW

Cevdet Kaynak et al. (2005) [1] investigated how changing the matrix and interface of a short carbon fiber reinforced diglycidyl ether of bisphenol-A (DGEBA)-based epoxy composite affected its mechanical performance. He observed that because silane coupling agent (SCA) treatment of carbon fiber surfaces improved the fiber's adherence to the matrix and load transfer efficiency, the mechanical characteristics of composite samples were also improved. The mechanical performance was also increased by using HTPB modification of epoxy matrix. Before mixing with the slurry, HTPB and hardener can be combined to vary the reaction's course. Chain extension may occur as a result of the hardener's reaction with the HTPB end groups, which increases the material's flexibility and toughness. Additionally, the epoxy matrix's creation of rubber domains enhances the material's flexibility and toughness. The usage of non-treated carbon fibers may have resulted in weak interfacial adhesion between the carbon fibers and epoxy matrix. Due to better interfacial adhesion, the mechanical characteristics of the fibers after SCA treatment increased. In particular, the epoxy matrix gained hardness from the inclusion of HTPB. When HTPB modification and SCA treatment were combined, the samples' mechanical performance improved the most.

P.F. Liu et al. (2012) [2] studied The complex failure mechanisms that are commonly regarded as the distinguishing feature of composites are becoming amenable to nondestructive testing advancement. The acoustic emission technique is used in this study to investigate the failure mechanisms and damage evolution of carbon fiber/epoxy composite laminates. The effects of

various lay-up patterns and hole sizes on the acoustic emission response are investigated in order to establish a mapping between failure properties and acoustic signal features such as energy, counting, and amplitude. Furthermore, the scanning electron microscope is used to observe and analyse the microscopic properties of various composite specimens after fracture (SEM). The mapping concept is used to control the microscopic failure mechanisms of composites such as splitting matrix cracking, fiber/matrix interface debonding, fibre pull-out and breakage, and delamination. The impact of complicated lay-up patterns and sizes on the damage and failure properties of composites is expected to be reflected by developing real mapping based on the acoustic emission approach.

Muhammad Akhsin Muflikhun et al. (2020) [3] evaluated the failure mode behavior of CFRP/ Adhesive/ SPCC hybrid thin laminates under axial and flexural loading for structural applications. For that, he utilized four different adhesives. Differential Scanning Calorimetry (DSC) and Fourier-transform infrared spectroscopy were used to characterize the materials (FTIR). An optical microscope was used to monitor surface behaviour both during and after the tensile test (final failure). DSC and FTIR measurements show that the materials go through the entire curing process. Tensile tests show that hybrid laminates containing SPCC can delay the early failure of CFRP laminates by up to 58.5%. The results show that the strain at failure increases by more than 13% from 1.85% for CFRP laminates to 2.1% for hybrid laminates. According to flexural testing, hybrid laminates are more flexible than CFRP laminates. When SPCC layers are added to CFRP laminates, the failure mechanism shifts from early fibre breaking to adhesive breakdown to final failure.

Geng Han et al. (2016) [4] conducted the failure analysis of carbon fiber reinforced composite subjected to low-velocity impact and compression after impact. The load in the direction of the thickness is extremely sensitive to composites, especially out-plane low-velocity impact (LVI). Experimentation and finite element analysis were used in his work to investigate the specific failure mechanisms of composite laminates composed of four different material systems (CCF300/Epoxy, CCF300/Bismaleimide, CCF800/Epoxy, and CCF800/Bismaleimide) when subjected to LVI and compression after impact (CAI). Intralaminar damage and interlaminar delamination are determined in a finite element model using cohesive elements and a newly proposed multi-scale failure criterion (MMF3), respectively. His experimentation and finite element analysis revealed that epoxy resin composites outperform bismaleimide resin composites in terms of damage tolerance, while CCF300 carbon fibre composites outperform CCF800 carbon fibre composites in terms of damage tolerance. The multi-scale failure analysis method accurately simulates the impact and CAI damage process of composite laminates.

Jong H Eun et al. (2021) [5] studied the effect of toughened polyamide-coated carbon fiber fabric on the mechanical performance and fracture toughness of CFRP. To increase the impact resistance and fracture toughness of carbon/epoxy composites used in his work, coatings of polyamide at various weight percentages (5 weight %, 10 weight %, 15 weight %, and 20 weight %) were applied. By using differential scanning calorimetry, X-ray photoelectron spectroscopy, and Fourier transform infrared spectroscopy, the chemical reaction between the polyamide and epoxy resin was investigated. The carbon/epoxy composites' mechanical characteristics and fracture toughness were examined. Impact tests, longitudinal flexural tests, and transverse flexural tests were used to examine the mechanical characteristics of the carbon/epoxy composites. An ultrasonic C-scan was conducted following the impact testing to

identify the internal damage location. Using a mode I test, the interlaminar fracture toughness of the carbon/epoxy composites was determined.

K Natarajan et al. (2015) [6] investigated how an ABS/PC thermoplastic blend may toughen a bifunctional epoxy (diglycidyl ether of bisphenol-A) matrix structure. By using melt-mix and particle dispersion techniques, a bifunctional DGEBA epoxy resin was 15% (w/w) modified with an ABS/PC thermoplastic blend. Two different types of blended products were compared that were both cured using a diamino diphenyl methane amine hardener under comparable conditions. He came to the conclusion that the ABS/PC thermoplastic blend improved the fracture toughness of the epoxy-DDM matrix system without Tg in general, and that the particle dispersion method was superior to the ABS/PC melt-mix method for producing greater fracture toughness.

Jacek Andrzejewski et al. (2020) [7] developed hybrid composites reinforced with a biocarbon/carbon fiber system and he did a comparative study for PC, ABS, and PC/ABS-based materials. Blends of this kind were used to lessen PC deterioration during the blending procedures, and it turned out that this was already successful at 40% ABS in the blend structure. The reduction of PC hydrolytic degradation caused by the addition of ABS to the matrix structure was validated by TGA analysis and rheological studies. While the peak values for the ABS/20BC sample were the same as the reference pure ABS, the DTG peak value for the PC/20BC composite decreased by 50°C. According to Izod studies, the impact resistance of ABS/BC composites was 37 J/m compared to 13 J/m for PC/BC materials. ABS was incorporated into the construction of PC/ABS composites to increase impact resistance. The major goals of the hybridized reinforcement application were to homogenize the fibrous CF

structures and lessen the material's thermal expansion. The difference in CLTE values between reference PC/20CF samples and PC/20(BC-CF) hybrid composites is about 1000% lower at under 300%. The isotropy of hybrid materials has significantly improved, as shown by a thorough examination of the expansion properties using TMA methods, which was further supported by structural observations. To reduce the phenomena of structure anisotropy, biocarbon might be a great supplement for standard fibrous reinforcement due to its improvement in process stability and outstanding thermomechanical parameters.

Ruifeng Liang et al. (2002) [8] did processing and characterization of recycled PC/ABS blends with high recycle content. To reduce batch-to-batch property changes in the compounded product, low molecular weight virgin PC was mixed with recycled PC to create a polycarbonate (PC)/acrylonitrile-butadiene-styrene (ABS) product with a high concentration of recycled PC. On a twin screw extruder, six PC/ABS blends were created by combining 50 weight percent virgin ABS, 0 weight percent low molecular weight virgin PC, and 25 weight percent high purity recycled PC retrieved from end-of-life devices. The rheological and mechanical characteristics of these mixtures were determined. Results indicated that this method might produce resin blends of consistently excellent quality and high recycling content. That is, his study has shown that a PC/ABS blend with a 40 weight percent recycled PC content, a 10 weight percent low molecular weight virgin PC content, and a 50 weight percent virgin ABS content would be an acceptable product with balanced processing and mechanical qualities.

Abhishek K. Pathak et al. (2016) [9] studied the mechanical properties of carbon fiber/graphene oxide-epoxy hybrid composites. The carbon fiber-graphene oxide epoxy resin-based composites show that the incorporation of GO in an epoxy matrix results in good

mechanical characteristics. At just 0.3 weight % of GO, the bending strength increases by 66% and the modulus by 70%. A 25% increase in interlaminar shear strength is seen. The enhancement in the mechanical properties of epoxy resin, the hydrogen bonding contact between reinforcement and matrix, and the mechanical interlocking of graphene oxide are all responsible for the rise in mechanical qualities. When GO content is very low, bonding around the reinforcements is improved by the high surface area of nanoscale GO, but increased GO content causes agglomeration in the matrix phase, which ultimately leads to bonding around the fibers. One strategy for enhancing the characteristics of carbon fiber polymer composites is the use of graphene oxide.

Prashanth Turla et al. (2016) [10] studied the interlaminar shear strength (ILSS) of glass and carbon fiber reinforced epoxy matrix hybrid composite. The interlaminar shear strengths of three different materials were evaluated: glass-carbon fibre reinforced epoxy matrix hybrid composite (three-phase composite), glass fibre reinforced epoxy matrix composite, and carbon fibre reinforced epoxy matrix composite (two-phase composites). Because of hybrid compositing, the value of the three-phase composite is significantly higher. In two-phase composite materials, the matrix material has a significant impact on the ILSS value.

K. Vijaya Kumar et al.'s (2017) [11] experiment was carried out to characterize of ILSS of CFRP laminates. However, because this combination has greater strength than the other laminates, it is deemed the master laminate. The experimentally discovered ILSS values for laminates with different fibre orientations proved to be different from the standard test laminate of 0/90 degree fibre orientation laminate. The discovered ILSS values were useful in determining the appropriate correction factor, that could then be multiplied by the ILSS value

of the test specimen to determine the exact strength of the actual part.This information aids the designers in creating the layup sequence for composite constructions with various orientations.

Binhua Wang et al. (2020) [12] is investigated based on the mode I crack growth test of a double cantilever beam, the interface toughness of aramid short fiber reinforced carbon fiber composite. Shorter fibres are more deeply buried in the resin-rich zone of carbon fibres, producing significant tension resistance and enhancing aramid fibre pull-out and peeling resistance. When a mode I crack spreads to aramid fibres in the resin bonding layer of a laminate, the tension resistance and grip force created by those fibres prevent the fracture from spreading. Furthermore, the longer peeling length of the aramid fibres has hampered the bridging effort. The critical energy release rate and average peak load of the bonding layer with 3mm aramid fibres have increased by 292.87% and 168.59%, respectively. The quantity of aramid fibres used in bridging is greater in 24 g/m2 specimens than in 12 g/m2 specimens, and thereinforcement effort of the former is likewise noticeably improved.

M.V. Gordić et al. (2007) [13] details an experimental investigation of the Mode I interlaminar fracture of composites made of unidirectional carbon fibers and epoxy resin. In a double cantilever beam (DCB) test, before and after gamma irradiation at different dosages, the energy release rate G_{IC} of the Mode I delamination strain was evaluated. Dynamic mechanical tests were used to calculate the epoxy matrix's glass transition temperature or T_g. SEM images of the delamination surfaces on the tested coupons were captured. The variations in G_{IC} values were linked to the variations in matrix or fiber/matrix dominated mechanical properties under irradiation, as well as with irradiation doses, T_g values, and delamination microfractographic features.

M.S. Sham Prasad et al. (2011) [14] studied experimental methods of determining fracture toughness of fiber reinforced polymer composites under various loading conditions. Interlaminar fracture testing for polymer-matrix composites has developed very slowly. It took almost ten years to standardize test procedures, even for Mode I loading. Due to crack branching and/or delamination that deviates from the core plane, multidirectional lay-ups commonly cause issues with Mode I loading. Both outcomes render the ASTM-compliant analysis incorrect. Additional loading modes and rate tests are also being developed. International agreement has not yet been reached as a consequence of early round-robin work on Mode II ENF done jointly by JIS, ASTM, and ESIS. Although Mode III fracture is crucial for edge delamination, substantially less research has been reported on it than on Mode I and Mode II fracture.

Hossein Saidpour et al. (2003) [15] used End-notched flexure (ENF) specimens to study the interlaminar fracture behavior of unidirectional carbon/epoxy composites under flexural pressure. Total fracture toughness energy at the highest stress the materials could withstand while still extending the delamination was used to compute G_{IIc} values. According to the findings, high-temperature molding systems (XHTM45) have GIIc values that are much above 1000 J/m^2. After post-cure, G_{IIc} has also grown noticeably for medium-temperature systems (MTM). The behavior of compressive strength after impact (CSAI) tests is somewhat correlated with that of G_{IIc} tests. A connection between the two test findings was also revealed by comparing the G_{IIc} levels with the CSAI. SEM Micrographs demonstrated their strong fiber/matrix interface and outstanding delamination resistance, making them effective crack stoppers. After post-curing at high temperatures, dynamic mechanical analysis (DMA) showed

that the T_g and modulus retention of the LTM and MTM prepregs had risen. For various tough matrix materials, the failure processes appear to vary and appear to be greatly influenced by the cure and post-curing circumstances. This is especially obvious for medium and low-temperature molding systems that cure at 135°C and 80°C.

Y He et al. (2013)[16] found that adding thermoplastics to epoxy (YD-128) and adding carbon fiber reinforcing assisted to change the material's different properties. For the modification of epoxy, they used three different types of thermoplastics (PEI, PC, and PBT). The reinforcing of carbon fiber in epoxy laminates was accomplished using vacuum-assisted resin transfer molding (VARTM). The thermoplastic percentage of the modified epoxy was up to 1.5wt%. Impact strength testing, morphological analysis, thermomechanical analysis, dynamic mechanical analysis, thermogravimetric analysis, and laminate microcracking were all part of their investigation. They discovered that the impact strength of the PEI-modified epoxy was 45% higher at cryogenic temperatures than it was for clean epoxy. The impact strength of PEI at room temperature was raised by 59%.On the other hand, at cryogenic temperatures, PC and PBT also increased the impact strength of the modified epoxy matrix. The impact strength rose to 1.5wt% when evaluated at room temperature before declining. The thermoplastic-modified epoxies had lower coefficients of thermal expansion (CTE) than the raw epoxy. When compared to plain epoxy, PBT, PEI, and PC modified epoxies' storage moduli were determined to be 5025 MPa, 4733 MPa, and 4539 MPa, respectively. Modified epoxy has a slightly higher glass transition temperature (T_g) than raw epoxy. Additionally, they looked examined how neat epoxy and modified epoxy behaved in microcracks. Based on their findings, they concluded that PEI and PC, due to their low CTE value and high impact strength, were particularly successful at preventing the development of microcracks during cryogenic thermal cycles.

Jyotishkumar et al. (2011) [17] studied the effect of curing on stress relaxation of prepared ABS/epoxy composites. The focus of the study is on how the cure schedule affects the final thermomechanical behavior of the epoxy and ABS blends. As 3.6, 6.9, 10, and 12.9 wt% of epoxy and the blend were made using the melt mixing procedure, the ABS concentration varied. Epoxy/ABS mixes' thermal, mechanical, and morphological characteristics were studied. They discovered that the ABS content increases the domain size and interparticle distance. The effectiveness of launching an energy-absorbing mechanism is measured by the domain size. Because ABS has a substantial coalescence effect at greater concentrations, it is discovered that inter-particle distances increase with ABS concentration. In light of this, the epoxy blend contains 3.6 wt.% ABS exhibits improved qualities in comparison to the other compositions. They added that the system's dimensional stability is impacted by the existence of internal stress. By using two-stage healing rather than one step, the internal stress can be relieved. Regardless of the curing schedule used, thermal and mechanical properties are comparable. However, because the thermoplastic is heterogeneous, blending with it alters the mechanical and morphological qualities.

Xiaole Cheng et al. (2017) [18] gives an overview of novel techniques for the preparation of different epoxy/thermoplastic blends. It is acknowledged that adding epoxy resins to thermoplastic resins necessarily increases resin viscosity. When creating epoxy/thermoplastic mixes with a relatively low thermoplastic percentage, liquid low-shear batch mixers are preferred. Highly viscous mixers, such as internal mixers or twin-screw extruders, are frequently employed for mixes containing a high proportion of thermoplastic, particularly when thermoplastics form a continuous matrix phase. Additionally, continuous mixers based

on twin-screw extruders offer more versatility to handle various component kinds and chemical compositions than batch mixers do. They can be utilized as continuous reactors to make cured epoxy/thermoplastic mixes in a single step because of this special advantage. For the preparation of epoxy/thermoplastic mixtures, non-mechanical techniques are equally crucial. Although solvent casting is an easy and efficient way to combine thermoplastic and epoxy, it is frequently used only in small-scale laboratory research because to cost, safety, and environmental concerns. Other cutting-edge approaches like RAM technology, in situ polymerization, and situ dissolution are particularly appealing since they effectively address the processing challenges brought on by the addition of thermoplastic without considerably altering the manufacturing processes. But it must be emphasized that each of these methods has a stringent chemical and thermoplastic compatibility requirement.

Yongsung Eom et al. [19] developed an experimental setup to observe void formation upon curing of epoxy resin. This demonstrated that voids originating at gelation can be determined by a crucial internal stress that is independent of the isothermal cure temperature. For stress-initiated voids, this critical value can be viewed as one of the material characteristics. The processing of composites was used with this outcome. The presentation of a process window aims to reduce internal stress levels and prevent void formation during cure. A novel model that took into consideration the pressure applied during cure was used to compute the internal stress. The crucial stress for void start was contrasted with this stress. In order to show the permitted applied pressure as a function of the fibre volume percentage and the architecture of fibre networks during cure, a process window was created.

CHAPTER 3

METHODOLOGY

3.1 SYNTHESIS FOR EPOXY MODIFICATION

The basic steps involved in the synthesis of epoxy modification are described as follows:

1. Cryo-grinding
2. Melt-mixing
3. Degassing

The overall setup of the epoxy modification is shown in figure 3.1

3.1.1 Cryo-grinding

The process of cooling or chilling a substance and then reducing it to a small particle size is known as cryogenic grinding, also known as freezer milling, freezer grinding, and cryo-milling. For instance, thermoplastics soften, adhere in lumpy masses, and clog screens when ground to small particle sizes at room temperature. The thermoplastics can be coarsely crushed into powders appropriate for electrostatic spraying and other powder operations when chilled by dry ice, liquid carbon dioxide, or liquid nitrogen.

For the cryogrinding set-up, a mechanical grinder is used. Liquid nitrogen is placed into the grinder, where it chills the PC and ABS pellets, causing them to be coarsely crushed into powder.

3.1.2 Melt-mixing

Melt mixing is used to blend the DGEBA epoxy resin YD-128 with the desired thermoplastics PC and ABS.

The majority of advantageous epoxy/thermoplastic mixtures are made by melt mixing and solvent mixing. Solvent mixing is a time-consuming, chemically unclean, and less environmentally favorable method [19]. Additionally, this method increases the chance of void development during curing, which can result in unanticipated failure [18]. Here, we use melt mixing because there are no chemicals that need to be left over while the product cures. Because it is among the simplest and cleanest methods for modifying epoxy and obtaining void-free samples [19].

Using a balance, 200g of epoxy is weighed into a silica mold. The composite exhibits enhanced mechanical characteristics when the total weight of the thermoplastics is 1.5 wt% [16]. Cryo-grinded PC and ABS powder are added to epoxy after it has been heated to roughly 180°C in a sand bath, which was swirled for 60 minutes, causing a mild yellowing of the modified epoxy. Using a trial-and-error method, the temperatures for melt-mixing PC, ABS, and PC/ABS into DGEBA were established using the color change of DGEBA during modification as the control parameter. To achieve the best possible blending of epoxy and thermoplastic, the system must be entirely agitated and mixed. To prevent overheating, the temperature is recorded often and kept between 180°C and 190°C. After allowing the modified resins to cool to room temperature, 100g of TH7301 was added, and everything was thoroughly mixed. A temperature-controlled sand bath is used to melt-mix PC, ABS, and PC/ABS into DGEBA, as shown in figure 3.1.

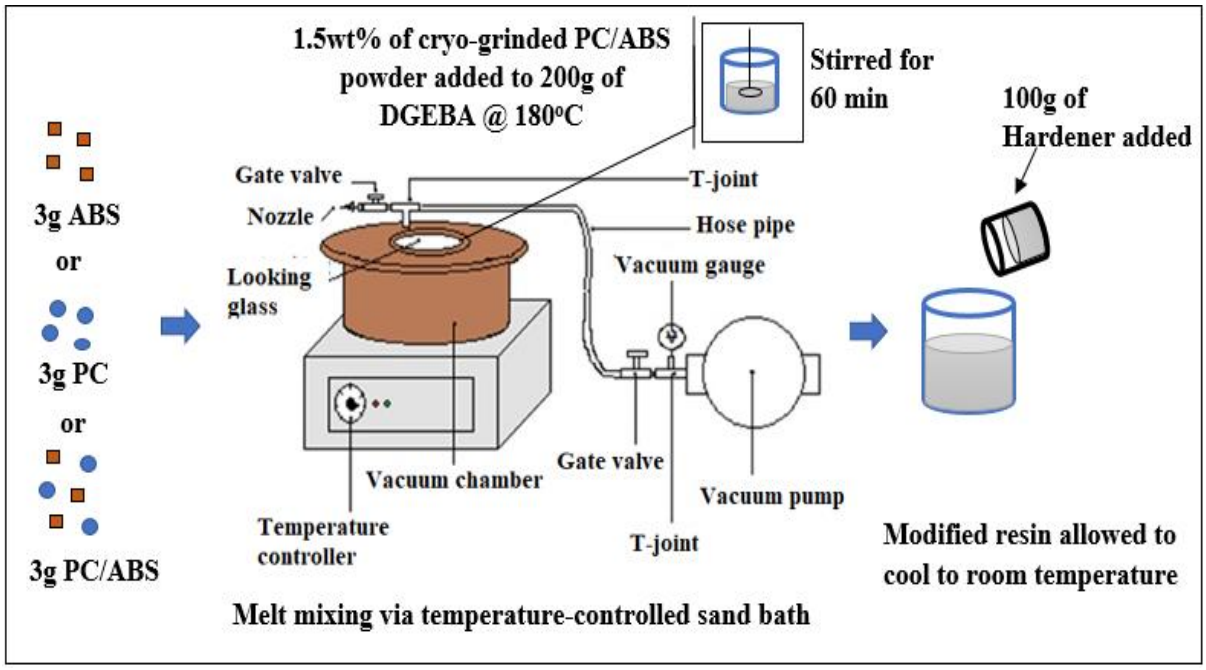

Figure 3.1 Epoxy modification

3.1.3 Degassing (Stabilizing of Resin/Hardener in vacuum degassing chamber)

The hardener and thermoplastic-modified epoxy are mixed in a 2:1 ratio, and the mixture must be degassed before fabrication. To get rid of any trapped bubbles that may have formed due to poor mixing with the hardener, the mixture must be degassed. Degassing is necessary because the entrapped bubbles create voids once the epoxy is cured, which causes the composite to fail suddenly under mechanical loading [21]. The modified epoxy hardener mixture is degassed using the following processes in the laboratory setup depicted in Figure 3.2.

- To prevent epoxy contamination during the degassing process, clean the vacuum chamber and top lid of dust and solid debris.
- The chamber is filled with a thoroughly mixed epoxy/hardener mixture, and the top lid is then fastened.
- Ensure that the top lid is securely seated and that the gaskets are completely sealed.

- Through a hose pipe, join the inlet port to the pump's suction side.
- Close the exhaust valve and open the inlet valve, then turn on the vacuum pump.
- When the necessary vacuum levels are reached, keep checking the vacuum gauge and shut the inflow valve.
- Close the valves to maintain the vacuum to some extent while allowing the trapped air to bubble up and burst.
- To get rid of all the unnecessary air inside the chamber, open the exhaust valve.
- To get a clear stabilized resin and to free all the trapped bubbles, periodically repeat the stages.
- Turn off the vacuum pump, remove the top lid and take the resin out for fabrication.

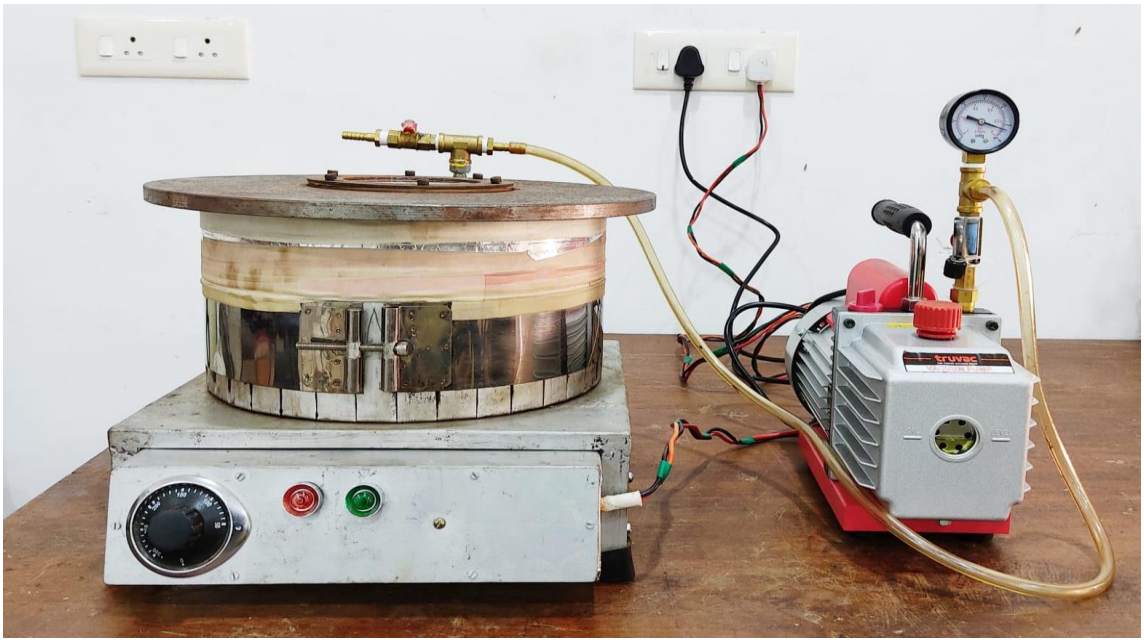

Figure 3.2 laboratory setup of Vacuum degassing unit

3.2 SPECIMEN PREPARATION

3.2.1 Carbon fiber lay-up

For carbon fabric, there is a relation existing between the thickness and weight of the fabric

Consolidated thickness (in mm) = Weight/1000 (Easy Composites, UK)

Weight of the carbon fabric = 220 g/m^2

Consolidated thickness for one layer of fiber = 220/1000 = 0.22 mm

The number of sheets of carbon fiber used = 15 numbers.

The thickness of 15 layers of carbon fiber sheets = 15×0.22 = 3.3 mm

Approximate/total thickness of the composite casted using VARTM = 3.7 mm

Number of epoxy layers = 16 layers

Thickness of 16 layers of epoxy layers = Approximate/total thickness of the composite

- Thickness of 15 layers of carbon fiber sheets

= 3.7 - 3.3 = 0.4 mm

$$\text{The thickness of one layer of epoxy} = \frac{\text{Thickness of 16 layers of epoxy layers}}{\text{Number of epoxy layers}}$$

$$=0.416 \quad = 0.025 \text{ mm}$$

The 3K, 22 twill weaved carbon fiber (CF) fabric cloth is cut into 15×15 cm squares for fabrication, and the surfaces of these squares are cleaned with acetone before being heated in an air oven to 100°C. Since each plie of the chosen CF fabric cloth has a nominal thickness of

0.22mm, a minimum of 15 plie lay-ups are needed for a 3mm thick CFRP laminate specimen. The lay-up is shown in figure 3.3.

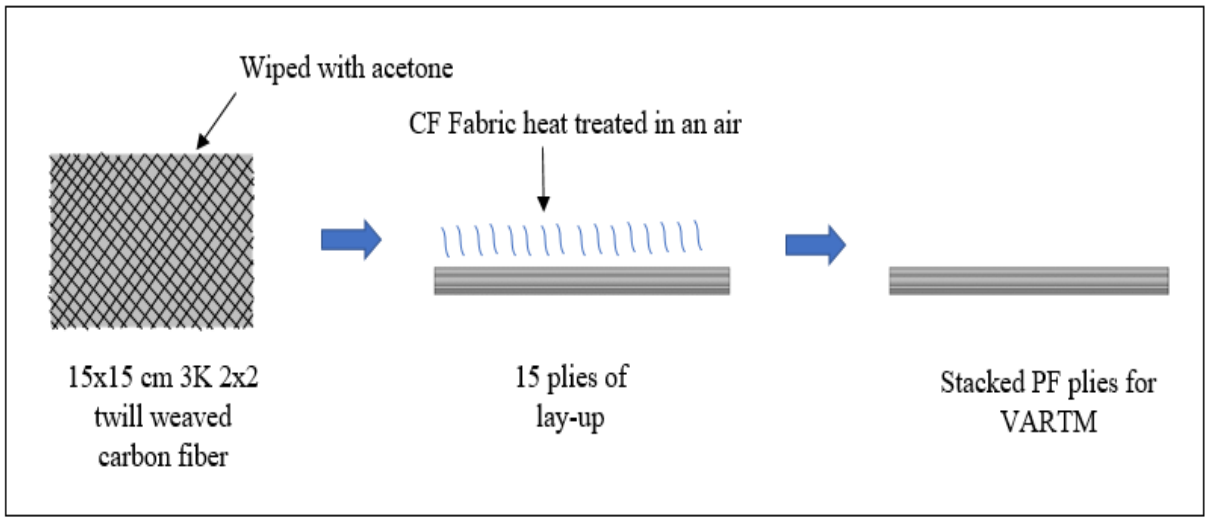

Figure 3.3 Carbon fiber lay-up

3.2.2 Vacuum-assisted resin transfer molding (VARTM)

Utilizing the VARTM process, neat and thermoplastic-modified epoxy composites are created. To guarantee superior surface finishing of the cast composite, a glass plate with the size 30cm × 30cm × 1cm is chosen for this. Wax is applied to the glass plate to prevent the mesh and carbon fiber from adhering to it. Injection of 8cm × 8cm mesh is positioned in the middle of the glass surface. Over the mesh, a peel-ply cloth with the necessary dimensions is positioned. Peel ply fabric and infusion mesh to make sure that the epoxy is perfectly wet throughout the composite. Then, 7.5cm × 7.5cm of twill weave carbon fiber sheet is cut into 15 layers, stacked together, and positioned atop the peel-ply cloth. Yet again, the peel-ply fabric and infusion mesh is positioned over the stacked carbon fiber sheets. Thus, as depicted in figures 3.3 to 3.5, the carbon fiber sheets are sandwiched between the mesh-peel ply layers.

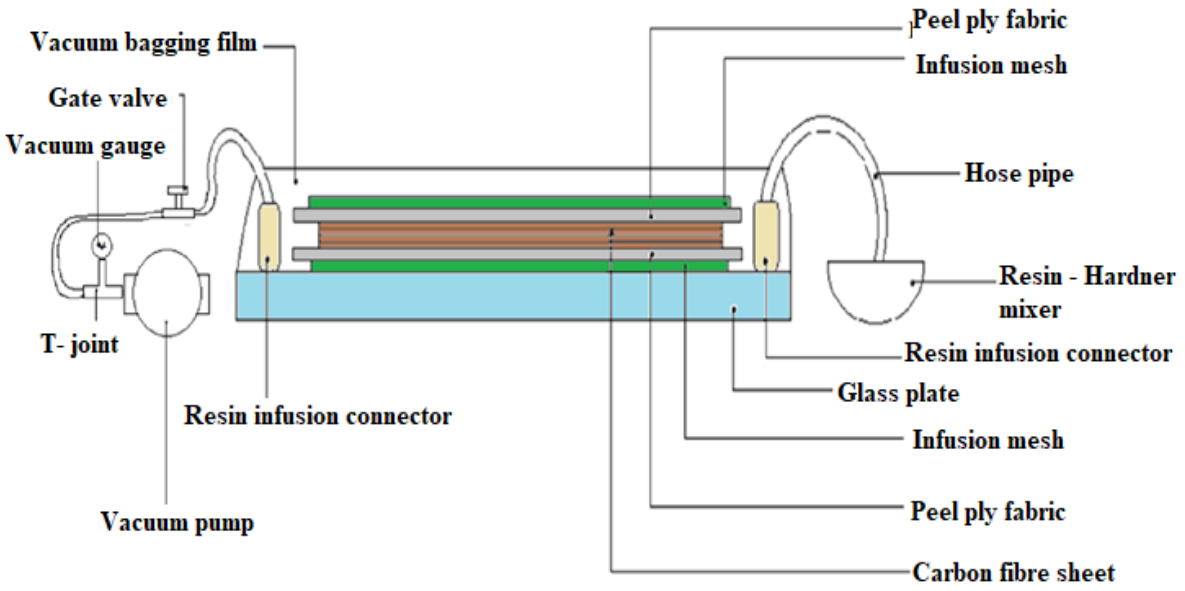

Figure 3.4 VARTM

Resin infusion connectors are positioned in the proper places to make it easier for the resin to enter the mold (inlet) and exit the mold (outlet). A vacuum bagging film is then placed over the entire arrangement. The vacuum bagging sheet is affixed to the glass surface using sealant tapes to ensure a proper vacuum. The resin pot and infusion connector are connected via hose pipes, allowing the resin to flow to the mold more easily. To create the vacuum inside the perfectly sealed bag, the vacuum pump is connected to the second infusion connector via hose tubing. Turn on the vacuum pump for a brief time and then turn it off to check for leaks. After making sure there are no leaks, inlet pipes are then submerged in the resin and the resin starts to flow. To regulate the resin flow rate and guarantee that the carbon fiber sheets are completely wet, gate valves on the outflow line are regulated. The resin begins to flow to the outlet pipes after thoroughly wetting the carbon sheets, and the gate valve is then shut fully. To prevent gas from leaking into the sealed bag, clamps are put on the inlet and outlet ports, and the vacuum pump is turned off. The fabricated composite is demolded after one overnight curing.

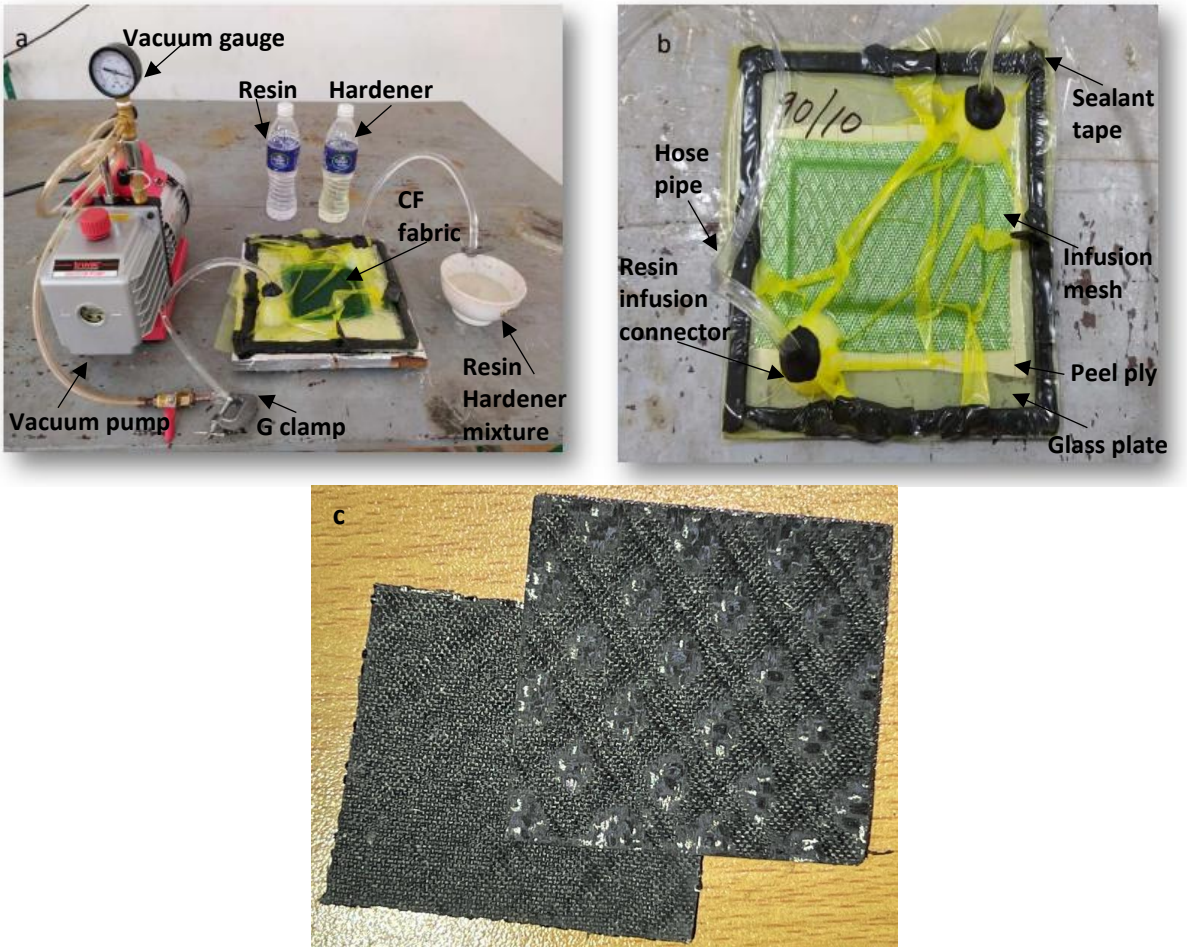

Figure 3.5 Composite preparation using VARTM, (a) laboratory setup, (b) mould surface after resin infusion, (c) fabricated composite sample

Table 3.1 Composite samples prepared (Thermoplastic content is 1.5 wt % of epoxy by weight) with 15 layers of CF sheets

Sl No	Composition
1	CF + Epoxy + Hardener (Neat)
2	CF + Epoxy/PC (100) + Hardener
3	CF + Epoxy/PC/ABS) (90/10) + Hardener
4	CF + Epoxy/PC/ABS (10/90) + Hardener
5	CF + Epoxy /ABS (100) + Hardener

CHAPTER 4

TESTING AND CHARACTERIZATION

4.1 MATERIAL USED

The thermoset polymer matrix epoxy with an epoxide equivalent weight (EEW) of 185 to 194 g/eq (YD 128, Aditya Birla Chemicals Ltd., Thailand) is chosen for the current study. Modified TH 7301 (Aditya Birla Chemicals Limited, Thailand), a cyclo aliphatic amine is a curing agent utilized. Melt mixing of thermoplastics like polycarbonate (PC, Makrolon 2856, Covestro AG, Germany) and poly (acrylonitrile butadiene styrene) is used to execute DGEBA matrix modification (ABS, Cycolac MG 47F, Sabic, Saudi Arabia). The composite material is reinforced with carbon fiber (3K genuine carbon fiber fabric cloth, 220g/m^2, 2x2 Twill Weave, Manufacturer Part No. CBC24030, Carbon black Composites, India).

4.1.1 Twill weave carbon fiber

Table 4.1 provides the information about the carbon fiber used in the present study as per the manufacturer (Carbon black composites, India)

Table 4.1. Properties of Carbon fiber

No.	Parameters	Specifications
1	Fabric type	3K genuine carbon fiber fabric cloth
2	Weave pattern	2 × 2 twill weave
3	Dimension	100cm × 30cm
4	Weight of the fabric	220 g/m^2
6	Izod impact strength	612 J/m

Fig. 4 Twill weave carbon fiber

4.1.2 Epoxy: YD 128

Table 4.2 provides information about the DGEBA-based epoxy YD 128 provided by the manufacturer, Aditya Birla Chemicals Ltd. Thailand.

Table 4.2. Properties of epoxy (YD-128)

No.	Property	Standard	Typical value
1	Appearance	Visual	Clear, colorless to light yellow liquid
2	Epoxy equivalent weight	ASTM D 1652-04	185 - 194 g/eq
3	Epoxide value	ASTM D 1652-04	5.15 – 5.40
4	Hydrolyzable chlorine	ASTM D 1726-03	0.05 max
5	Flash point	ASTM D 93	252℃
6	Density at 25℃	ASTM D 1475-98	1.16 g/ml
7	Viscosity at 25℃	ASTM D 2196-05	11,000 – 14,000 cPs

Fig. 4.2 epoxy YD-128

4.1.3 Hardener: TH 7301

The chosen epoxy's curing agent is TH 7301. Table 4.2 below lists properties of TH 7301 as per the manufacturer, Aditya Birla Chemicals Ltd., in Thailand.

Table 4.3. Properties of Hardener (TH 7301)

No.	Property	Standard	Typical value
1	Appearance	Visual	Clear, light yellow liquid
2	Odor	---	Amine
3	Amine value	DIN 16945	260 – 285 mg KOH/g
4	Flash point	ASTM D 93	100℃
5	Glass transition temperature	DIN 11357	50℃
6	Density at 25℃	ASTM D 1475-98	1.03 g/cc
7	Pot life at 25℃	TEC-AS-P-111	28 – 45 min

Fig.4.3. Hardener TH 7301

4.1.4 Poly (acrylonitrile butadiene styrene) (ABS)

Properties of ABS (cycolac MG47F resin) as provided by the manufacturer (Sabic, Saudi Arabia) are listed in table 4.4.

Table 4.4. Properties of ABS

No.	Property	Standard	Typical value
1	Specific gravity	ASTM D 792	1.04
2	Coefficient of thermal expansion	ASTM E 831	8.82E – 05 /°C
3	Notched Izod impact strength	ASTM D 256	320 J/m
4	Vicat softening temperature	ISO 306	98°C
5	Tensile stress at yield	ISO 527	47 MPa
6	Tensile strain at break	ASTM D 638	25 %
7	Melt temperature	---	220 - 260°C

Fig.4.4. ABS

4.1.5 Polycarbonate (PC)

Properties of PC (Makrolon 2856) as provided by the manufacturer (Covestro, Germany) are listed in table 4.5.

Table 4.5. Properties of PC

No.	Property	Standard	Typical value
1	Specific gravity	ASTM D 792	1200 kg/m^3
2	Coefficient of thermal expansion	ISO 11359-1, -2	0.65 × 10^{-4}/°C
3	Notched Izod impact strength	ISO 7391/b.o. ISO 180-A	70P KJ/m^2
4	Glass transition temperature	ISO 11357-1, -2	145°C
5	Tensile stress at yield	ISO 527-1,-2	65 MPa
6	Tensile strain at break	b.o. ISO 527-1,-2	130 %
7	Flexural stress	ISO 178	97 MPa
8	Melt temperature	---	280 - 320°C

Fig.4.5 PC

4.1.6 Glass mold

To get a better surface smoothness, the glass plate is employed as the casting surface for composites. The specifications are given in Table 4.6

Table 4.6. Specifications of glass

No.	Parameters	Specifications
1	Material	Glass
2	Size	30 cm × 30 cm
3	Thickness	10 mm
4	Manufacturer	Saint Gobain glasses

Fig.4.6 Glass mold

4.1.7 Mould release agent

To prevent materials from adhering to one another, the mould release agent is placed on the surface of the mould. Table 4.7 lists specifics of the mould releasing agent.

Table 4.7. Details of Mould release agent

No.	Parameters	Specifications
1	Form	Wax type
2	Colour	White
3	Max. operational temperature	Up to 200℃
4	Manufacturer	Carbon black composites

Fig 4.7 Mould release agent

4.1.8 G Clamp

After the resin infusion process, G clamps are utilized at the inlet and outlet hose pipes to stop air from spilling into the vacuum bag. Details of the G clamp are listed in Table 4.8

Table 4.8 details of G Clamp

No.	Parameters	Specification
1	Type	G clamp
2	Material	Iron
3	Brand	KETSY, India

Fig.4.8 G Clamp

4.1.9 Infusion mesh

Infusion mesh is a consumable component used to facilitate proper impregnation of fabrics during infusion processing or VARTM procedures by boosting the resin's sliding inside the vacuum bag (Vacuum Assisted Resin Transfer Molding). The mesh proves to be exceptionally effective for big moulds and/or medium-viscosity resin infusions when applied on corners and remote sections of the mould or throughout its whole surface in places with a high number of layers. Details of the infusion mesh are listed in Table 4.9

Table 4.9 details of infusion mesh

No.	Parameters	Specification
1	Provider	CF Composites, Delhi, India
2	Material	HDPE
3	Width	1500 mm
4	Color	Green

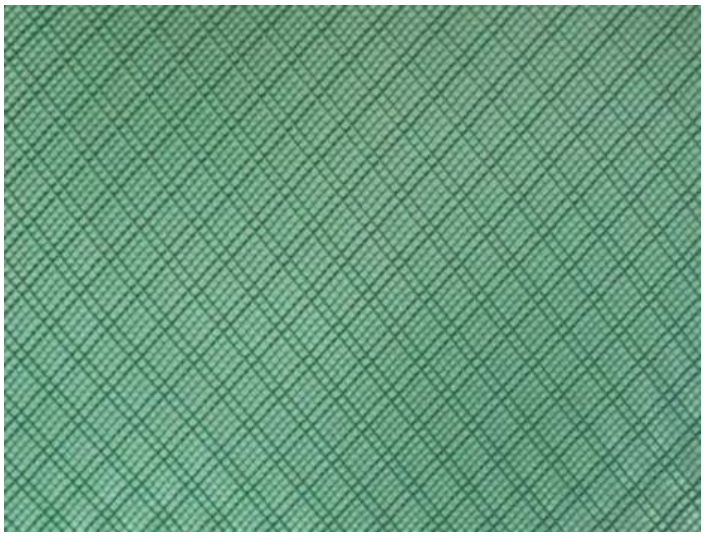

Fig.4.9 Infusion mesh

4.1.10 Peel ply fabric

Peel ply fabric's porous and woven construction allows it to absorb surplus resin and make sure the carbon fiber laminates are completely wet. Up until the patch is removed, it can stop substantial contamination of the patch surface. The peel ply should theoretically remove a very thin layer of resin from the composite to produce a brand-new, spotless surface. Details of the peel ply fabric are listed in table 4.10.

Table 4.10 Details of Peel ply fabric

No.	Parameters	Specification
1	Provider	CF Composites, Delhi, India
2	Material	Nylon 6
3	Color	Natural white
4	Tracer yarn material	Polyester
5	Thickness	85 GSM
6	Width	1000 mm

Fig.4.10 Peel-ply fabric

4.1.11 Vacuum bagging film

The preform is covered with a vacuum bag, and the pressured resin is then injected into the cavity with the help of a vacuum. Vacuum bags are prepared by attaching the glass mould to the vacuum bagging film so that a vacuum can be pulled. The details of Vacuum bagging film are given in Table 4.11

Table 4.11 Details of vacuum bagging film

No.	Parameters	Specification
1	Provider	CF Composites, Delhi, India
2	Material	Modified nylon resin film
3	Thickness	75 micron
4	Width	1000 mm

Fig.4.11 Vacuum bagging film

4.1.12 Sealant tape

Utilizing a sealant tape to adhere vacuum bagging sheets to the surface of the mould offers a better airtight seal when the vacuum is applied. Sealant tape is crucial because even the smallest leaks might result in the creation of voids in the composite. Table 4.12 contains a description of the sealant tape that was used for the VARTM in this study.

Table 4.12 Details of Sealant tape

No	Parameters	Specifications
1	Provider	CF Composites, Delhi, India
2	Material	Butyl-sealant tape
3	Dimension	3 mm × 15 mm × 15 m

Fig.4.12 Sealant tape

4.1.13 Resin infusion connector

The specifics of the connectors, which are listed in table 4.13, are used to join the hose pipe to the vacuum bag.

Table 4.13 Details of Resin infusion connector

No	Parameters	Specifications
1	Provider	CF Composites, Delhi, India
2	Material	PVC
3	Dimension	8 mm dia.

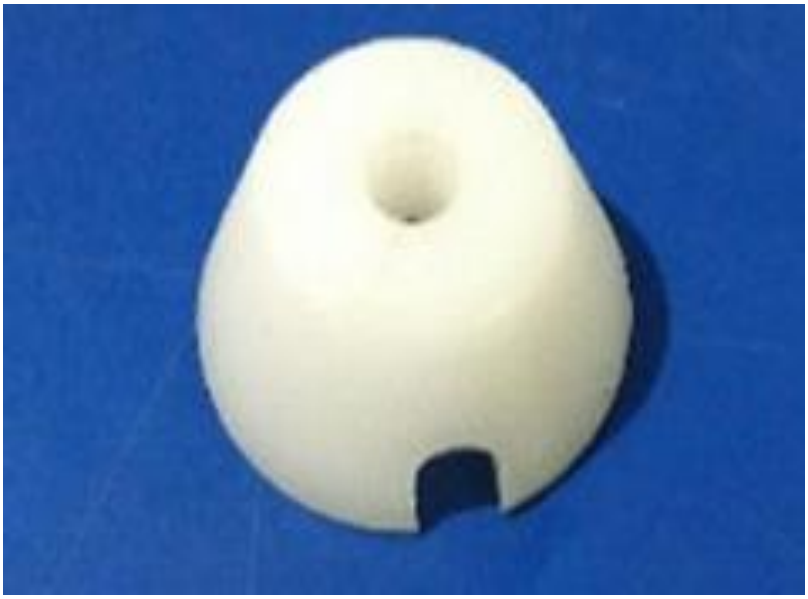

Fig.4.13 Resin infusion connector

4.1.14 Hose pipe

By connecting the vacuum bag to the pump, hose pipes are utilized to facilitate resin flow into and out of the vacuum bag as well as to create a vacuum inside the bag. Table 4.15 lists the hose pipe's specifications.

Table 4.1 Details of Hose pipe

No	Parameters	Specifications
1	Provider	CF Composites, Delhi, India
2	Material	PVC
3	Dimension	8 mm dia., 30 m length

Fig.4.14 hose pipe

4.1.15 Vacuum pump

A vacuum is created inside the vacuum bagging using a vacuum pump, which allows the resin to be infused into the mould. Table 4.15 includes information regarding the vacuum pump.

Table 4.1 Details of vacuum pump

No	Parameters	Specifications
1	Manufacturer	Truvac
2	Capacity	2.5 CFM
3	Weight	12.6 Kg
4	Dimension	336 mm × 123 mm × 255 mm
5	Displacement	113 L/min
6	Voltage	220 V
7	Frequency	50 Hz
8	Oil Capacity	220 ml
9	Stage	Double
10	Ultimate vacuum	50 microns

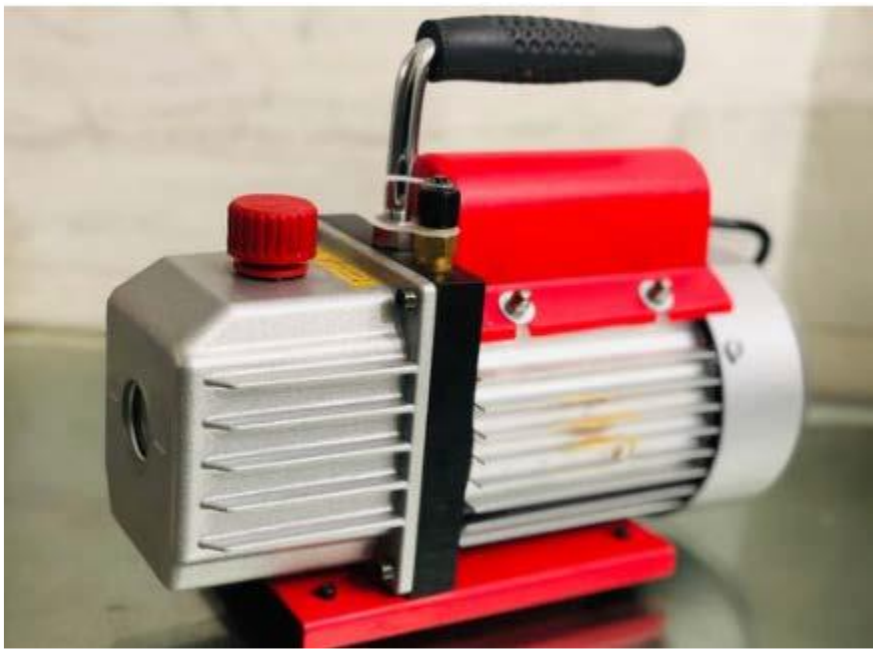

Fig.4.15 Vacuum pump

4.1.16 Mechanical grinder

The mechanical grinder is used for a cryo-grinding setup. The details of the mechanical grinder are given in Table 4.16

Table 4.16 Details of mechanical grinder

No	Parameters	Specifications
1	Brand	NILSAN
2	Color	Silver
3	Model	NSG100A
4	Material	Stainless steel
5	Power	650 W
6	Voltage	220 V
7	Rotate Speed	28000 RPM

8	Capacity	100 g
9	Type	Portable
10	Weight	2.6 Kg

Figure 4.16 mechanical grinder

4.2. CHARACTERISATION

4.2.1 FTIR Spectroscopy

It was confirmed that the curing reaction was finished by FTIR (Fourier transform infrared) analysis. With the aid of two FT-IR spectrometers from Perkin Elmer, the fully cured specimens were scanned via the attenuated total reflection (ATR) contact sampling method as per ASTM D5477. The spectra of each interferogram are generated as percentage transmittance against wavenumber after signal averaging 28 scans at a resolution of $4cm^{-1}$.

4.2.2 Thermo gravimetric analysis

Thermogravimetric analysis (TGA) is being used to examine the thermal stability of composite materials at various temperatures. Using a TGA Q 500 V6.7 Build 203 instrument, it is carried out between 25°C to 600°C at a heating rate of 10°C/mm. Each composite sample's 10- 20 mg weight is employed in the test. The test is carried out at Cornell University's Center for Materials Research (CCMR), in the United States as per ASTM E1640.

4.2.3 Differential scanning calorimetry (DSC)

Differential scanning calorimetry can identify changes in material properties at precise temperatures, exposing significant transition ranges and deterioration points. This is accomplished by taking accurate measurements of heat capacity and temperature. It is using DSC204F1 Phoenix from NETZSCH at a heating rate of 10 K/min, between -20^{o}C to 200^{o}C as per ASTM E1356.

4.2.4 Tensile test

The force necessary to break a polymer composite specimen and the extent to which the specimen stretches or elongates to that breaking point are measured using ASTM D3039 tensile testing. A stress-strain diagram generated by tensile tests is used to calculate the tensile

modulus. The test is carried out at FAN services - Advanced Materials Testing & Research Lab, Maharashtra, India.

4.2.5 Mode I, II, and Mix mode Analysis

To find Interlaminar Shear Strength (ILSS) and Strain Energy Release Rate (SERR), a Mode of failure analysis is used. Here Mode I, II, and mix-mode analysis are carried out as per ASTM D6671 at FAN services - Advanced Materials Testing & Research Lab, Maharashtra, India.

4.2.6 Scanning Electron Microscopy

Scanning Electron Spectroscopy (SEM) analysis is employed to assess the morphology of the fractured specimens after the mode of failure analysis. SEM images of the neat and PC/ABS modified epoxy composites are analyzed and studied. The test is carried out at FAN services - Advanced Materials Testing & Research Lab, Maharashtra, India.

CHAPTER 5

RESULTS AND DISCUSSION

5.1 FTIR SPECTROSCOPY

It was confirmed that the curing reaction was finished by FTIR analysis. In a chemical interaction with DGEBA epoxy, PC, ABS, and PC/ABS, it becomes partially soluble in DGEBA. The thermoplastics, PC, ABS, and PC/ABS blends in the DGEBA are seen to undergo a chemical reaction with the epoxide groups after being melt-mixed at processing temperature. As a corollary, the uncured modified DGEBA resin has a faint yellow hue. The characteristic curve of neat DGEBA, ABS, and PC/ABS is altered by the presence of PC, demonstrating the change in the chemical structure of DGEBA upon melt-mixing as shown in figure 5.1. The fact that there was no presence of the typical epoxy peak at 913 cm^{-1} indicates that all of the epoxy monomers were involved in the curing procedure. The characteristic peak at 913cm^{-1} is absent in the final cured composite when PC, ABS, or a hybrid blend of PC/ABS (90/10 or 10/90) are present, implying that the blend modification had no impact on the curing reaction. The absence of a peak at 913cm^{-1} in the FTIR analysis, as shown in figure 5.1, implies that only complete cross-linking was necessary to achieve the epoxy network's full range of property achievement.

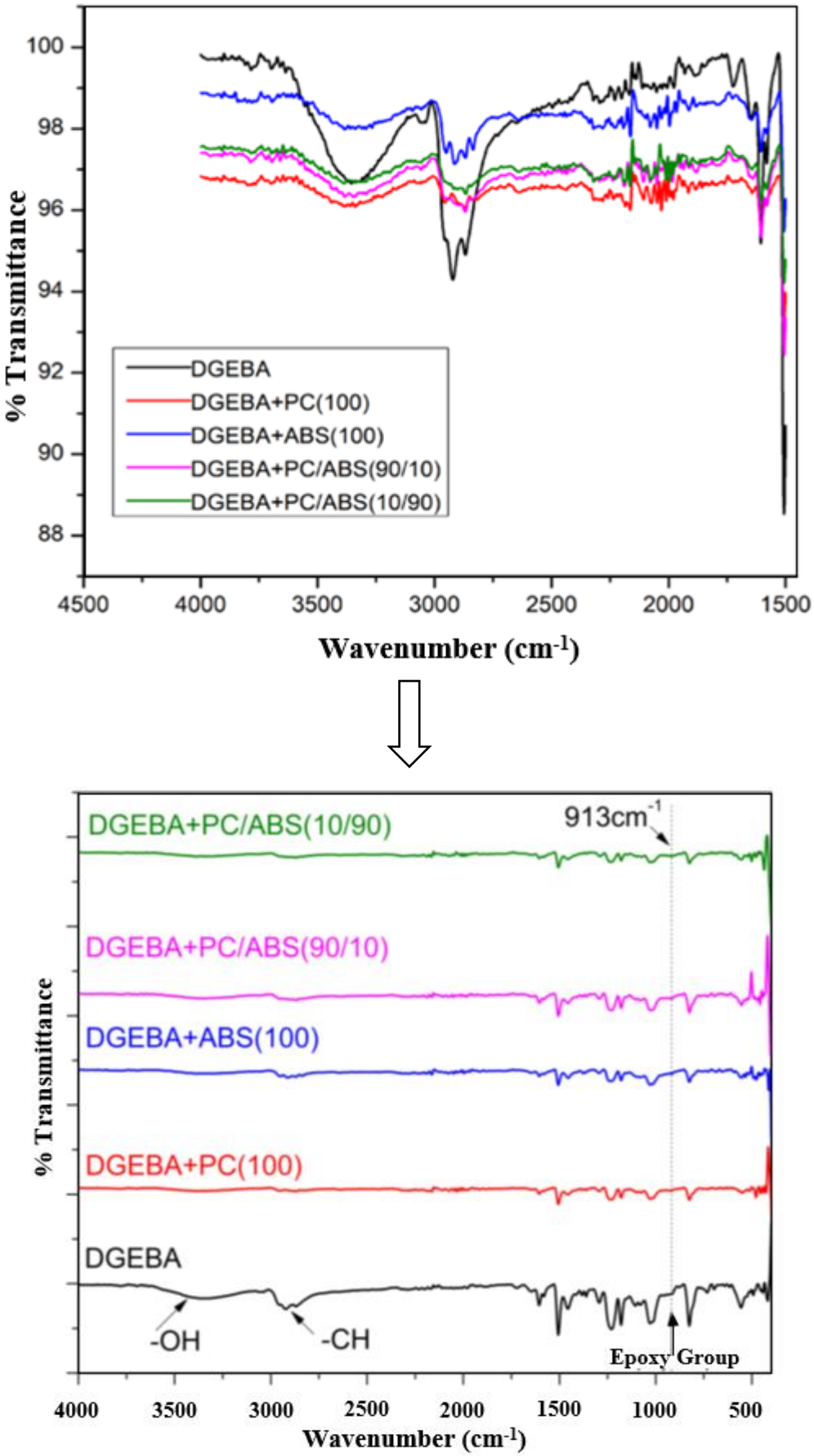

Fig. 5.1 FTIR overlay of DGEBA and modified DGEBA and CF composites

5.2 THERMOGRAVIMETRIC ANALYSIS (TGA)

To investigate the thermal stability of the composite at various temperatures, a thermodynamic analysis is carried out. Figures 5.2 to 5.6 show the TGA graphs of the neat and thermoplastic-modified epoxy composites (PC/ABS - 100/0, 90/10, 10/90, 0/100). The specimen from each composite sample is heated to temperatures ranging from 25 °C to 600 °C, and weight loss at various temperatures is analyzed. Figure 5.7 also includes an overlay graph of the TGA curves of plain and thermoplastic (PC/ABS) modified epoxy composites, which makes the comparative stabilities of the composites more explicit.

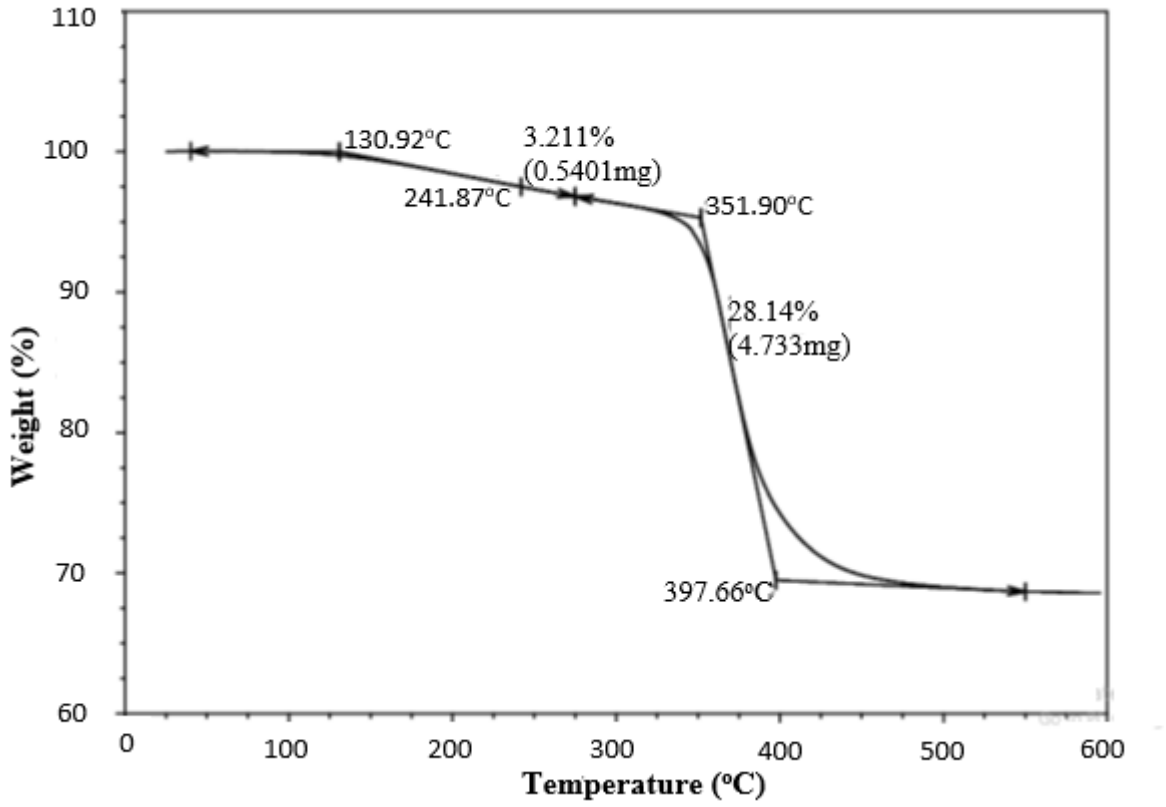

Fig. 5.2 TGA curve of the neat epoxy composite

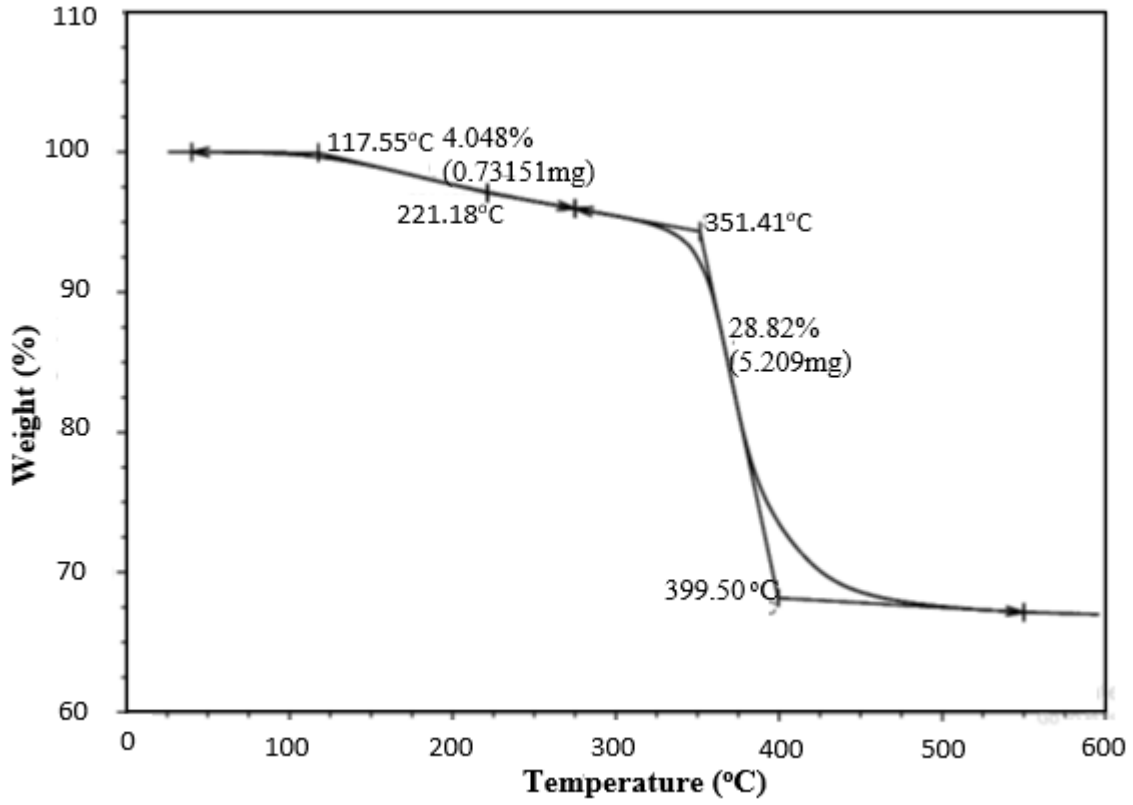

Fig.5.3 TGA curve of PC/ABS (100/0) modified epoxy composite

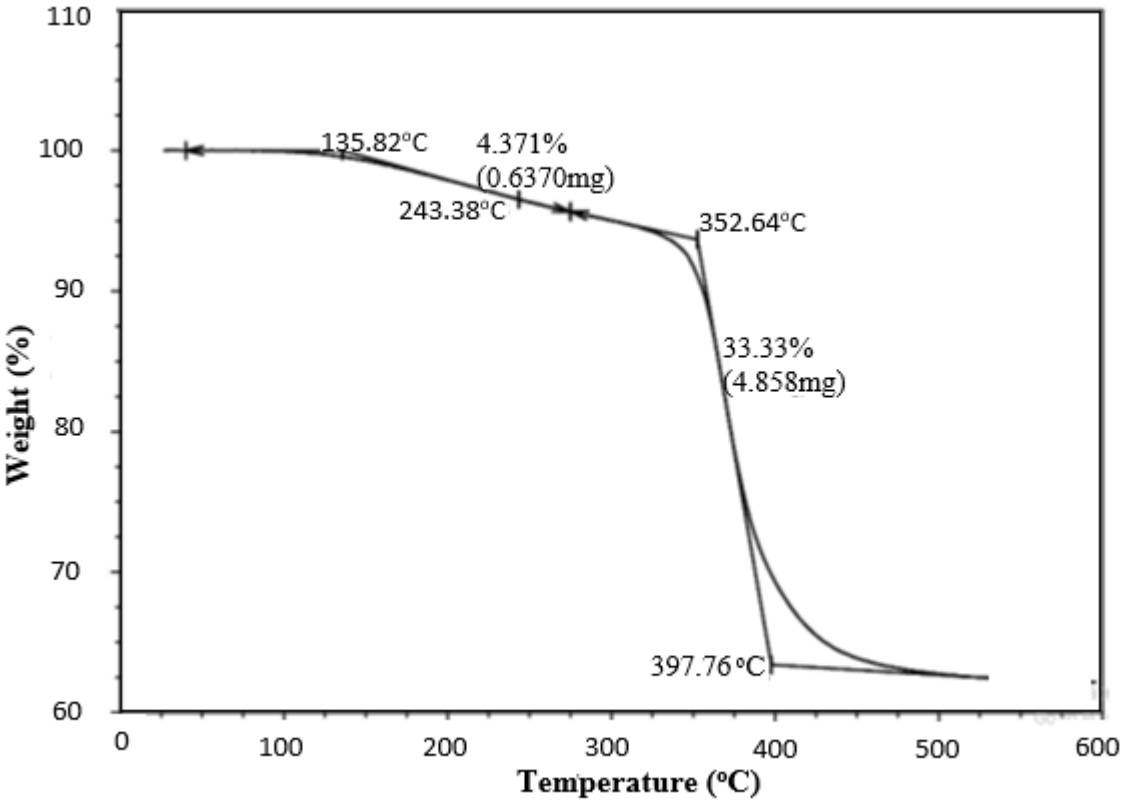

Fig.5.4 TGA curve of PC/ABS (0/100) modified epoxy composite

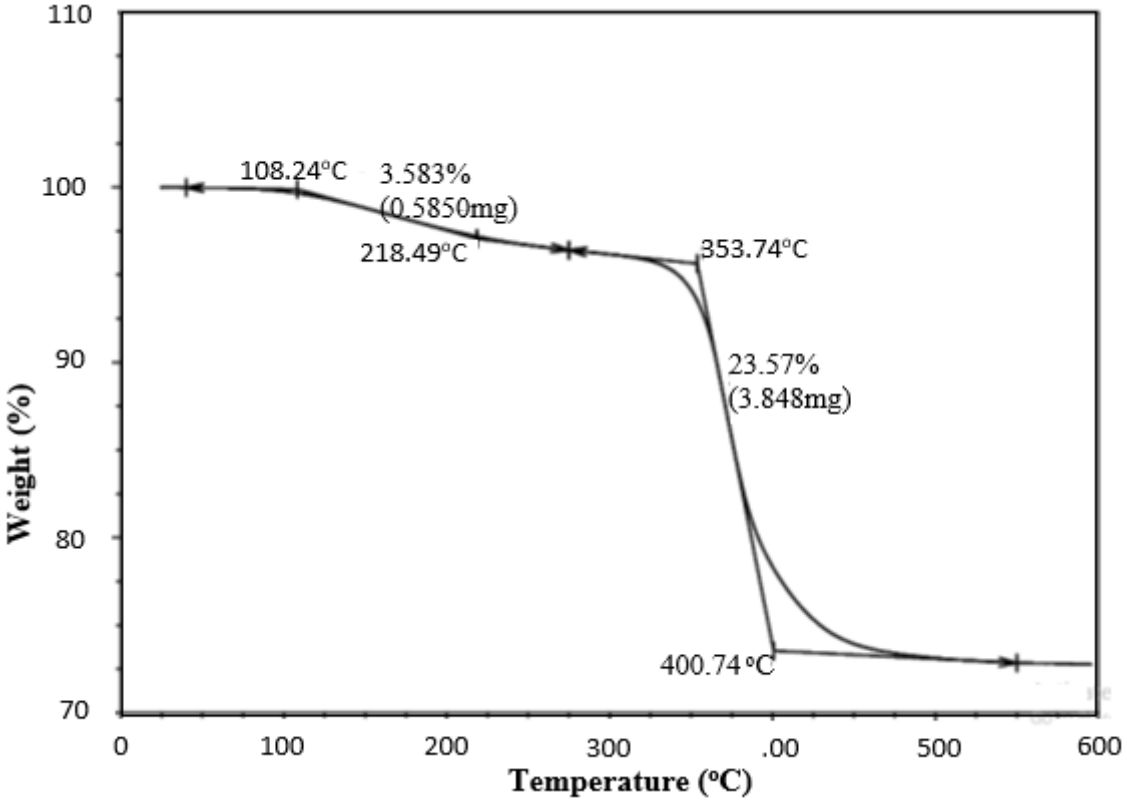

Fig.5.5 TGA curve of PC/ABS (90/10) modified epoxy composite

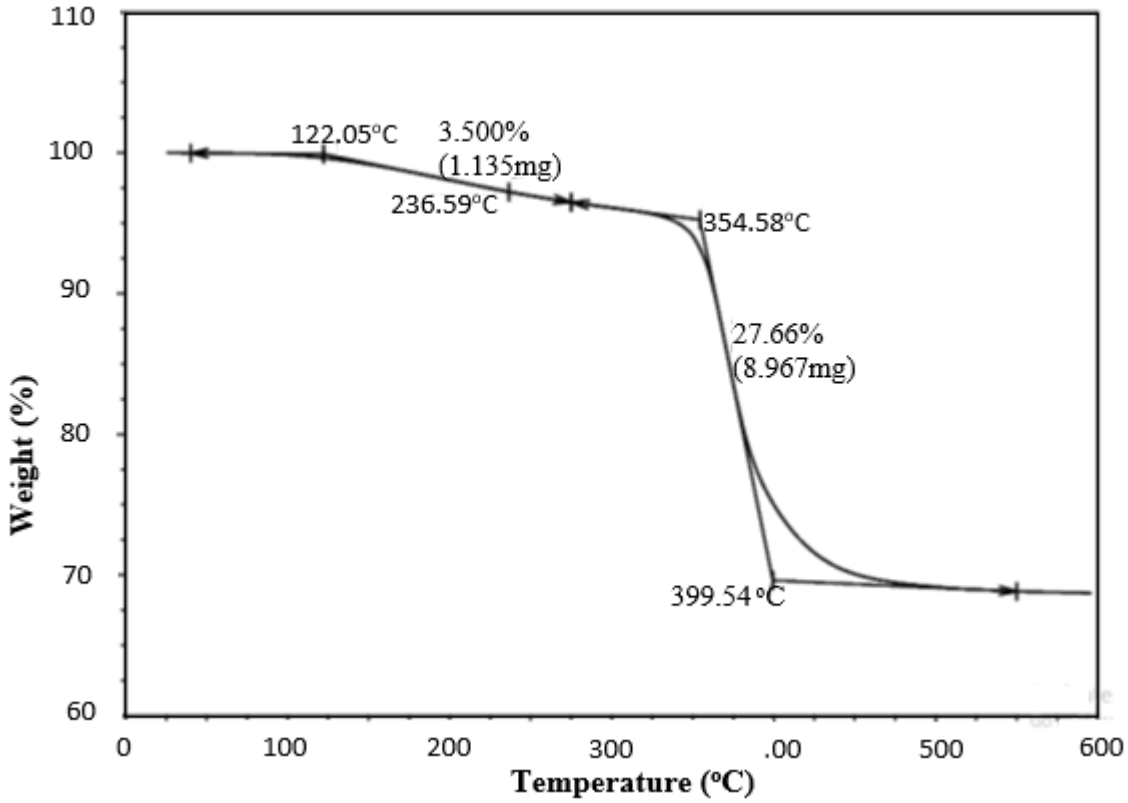

Fig.5.6 TGA curve of PC/ABS (10/90) modified epoxy composite

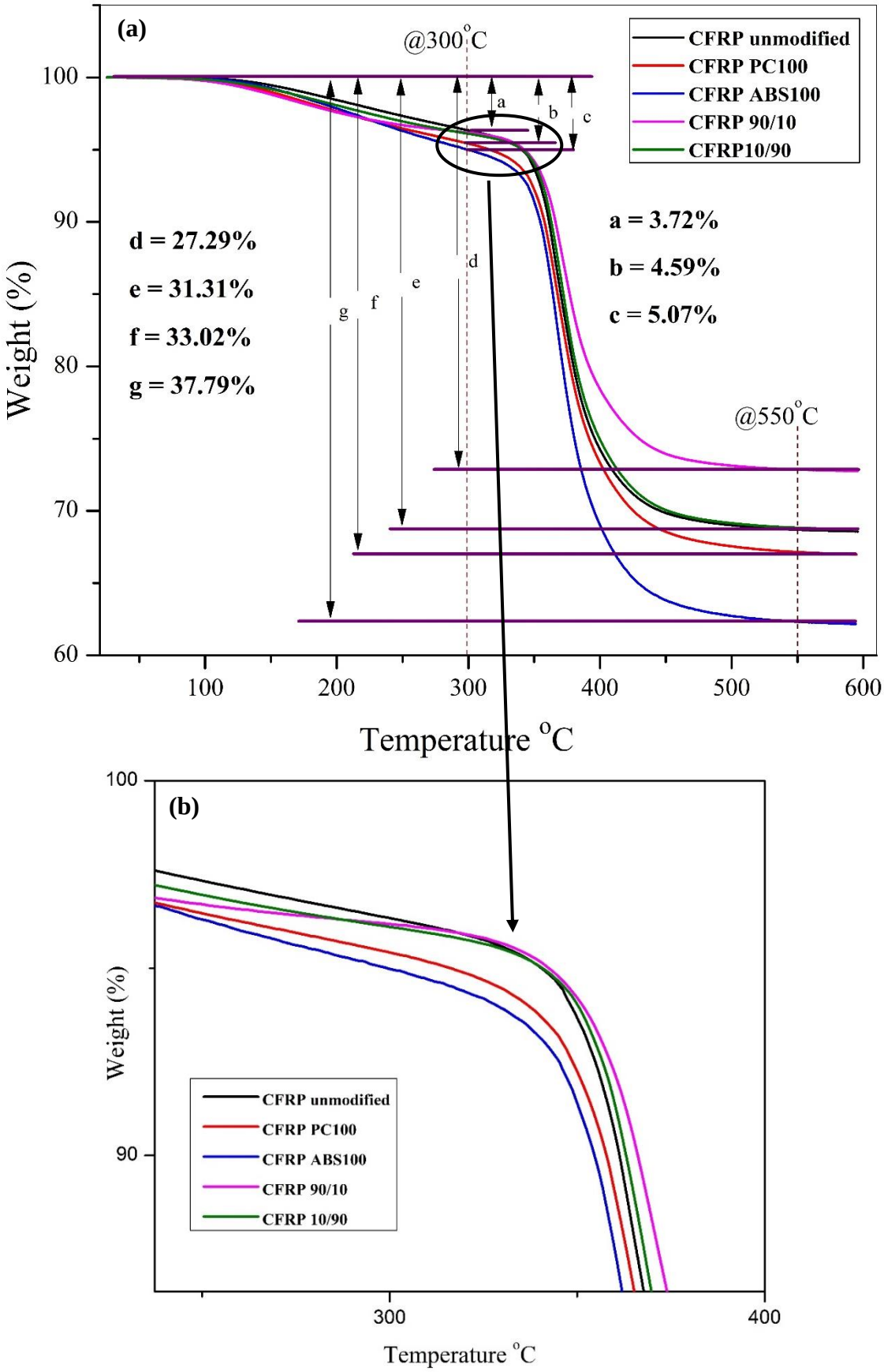

Fig.5.7 TGA curve (a) overlay and (b) zoomed portion of first degradation point at 350°C

Epoxies modified with PC/ABS [(100/0), (0/100), (90/10), and (10/90)] and pure epoxy lose weight (weight loss) at 350 °C at rates of 6.3%, 7.58%, 8.23%, 5.87%, and 5.91%, respectively (Table 5.1). It is evident from the weight loss of composites across a wide temperature range that the PC/ABS modified epoxy composites with blend compositions of 90/10 and 10/90 exhibit greater thermal stability than the neat epoxy composite. Around 350°C, when matrix breakdown begins, abrupt decreases in the curve are seen [16]. Additionally, it should be noted that the PC/ABS 90/10 blend composition has the highest residual weight following full disintegration at temperatures between 400°C to 600°. The stronger bond between the matrix and fiber as a result of the development of semi-interpenetrating polymer networks may be the cause of the improved stability [20].

The TGA results show that the PC/ABS (90/10) blend composition has enhanced the composite's thermal stability, however, the weight loss of the PC/ABS (100/0) and PC/ABS (0/100) modified composites is more than that of the unmodified (neat) epoxy composite.

Table 5.1: TGA data showing weight loss at 350^{o}C for DGEBA and modified DGEBA epoxy/CF composites

Sample	**Temperature**	**Weight loss (%)**
DGEBA	350	6.3
PC modified DGEBA + CF		7.58
ABS modified DGEBA + CF		8.23
PC/ABS (90/10) modified DGEBA + CF		5.87
PC/ABS (10/90) modified DGEBA + CF		5.91

5.3 DIFFERENTIAL SCANNING CALORIMETRY (DSC)

In comparison to PC and ABS-modified DGEBA epoxy, the PC/ABS blend (90/10 and 10/90) modified DGEBA exhibits increased bonding strength with CF. It is also important to note that when PC and ABS are added to DGEBA, the specific heat capacity (Cp) values for CFRP composites decrease by 52% and 86%, respectively, when compared to unmodified CFRP composites. While Cp exhibits an enhancement of 36.3% and 13%, respectively, in the cases of 90/10 and 10/90 modified DGEBA/CF composites. The enhancement in Cp might be the result of stronger bonds that were demonstrated as a result of the synergistic interaction or synergism effect between PC/ABS-modified DGEBA epoxy and CF. Even after complete thermal deterioration, 90/10 modified CFRP composites retain the highest weight percentage, that is 72.77%, followed by unmodified and 10/90 modified CFRP (68.75%), CFRP PC100 (67.04%), and CFRP ABS100 with the lowest value (62.27%). The decomposition rate of the 90/10 modified CFRP is interestingly slower than that of the other examples, indicating a positive synergism effect at work.

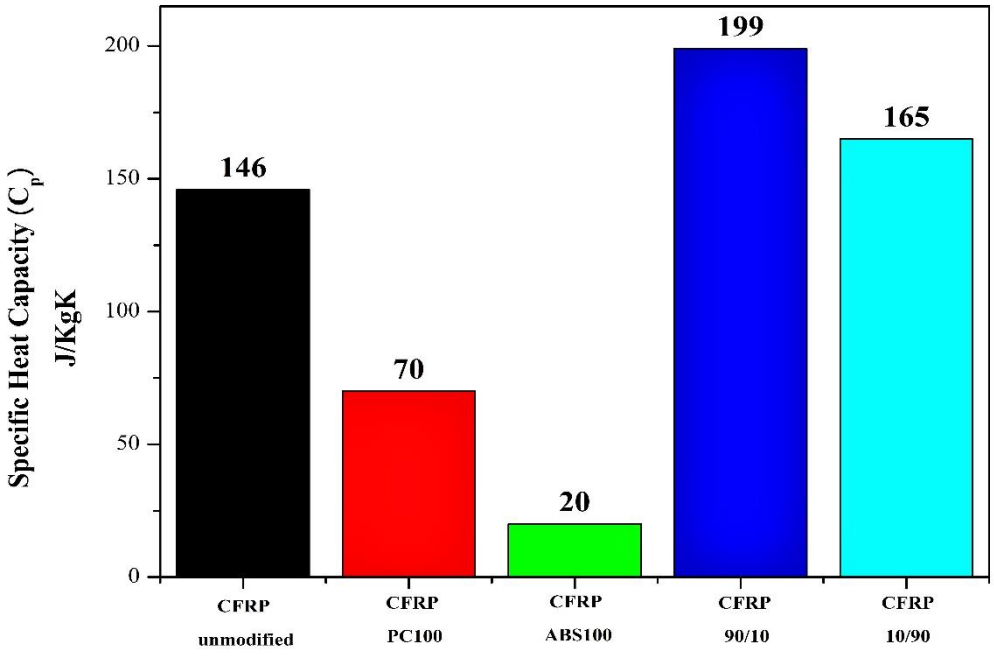

Figure 5.8 Specific heat capacity values of modified CFRP compared with unmodified CFRP

Figure 5.8 shows a contrast of the unmodified CFRP's specific heat capacity values with those of unmodified CFRP.

To ensure greater interlaminar strength, 90/10 demonstrates a synergism effect in boosting the thermal stability of CFRP composites with better adhesion.

5.4 TENSILE TEST

For DGEBA to be used in a broad range of applications, a reduction in its brittle characteristics is a crucial feature. To do this, 90/10 modified CFRP composites and unmodified CFRP are evaluated for ultimate tensile stress and elongation at break values. Figure 5.9 and figure 5.10 shows that the average elongation values at the break for 90/10 modified CFRP composites demonstrate a 17.3% increase (10.4mm to 12.2mm) in comparison to unmodified CFRP composites.

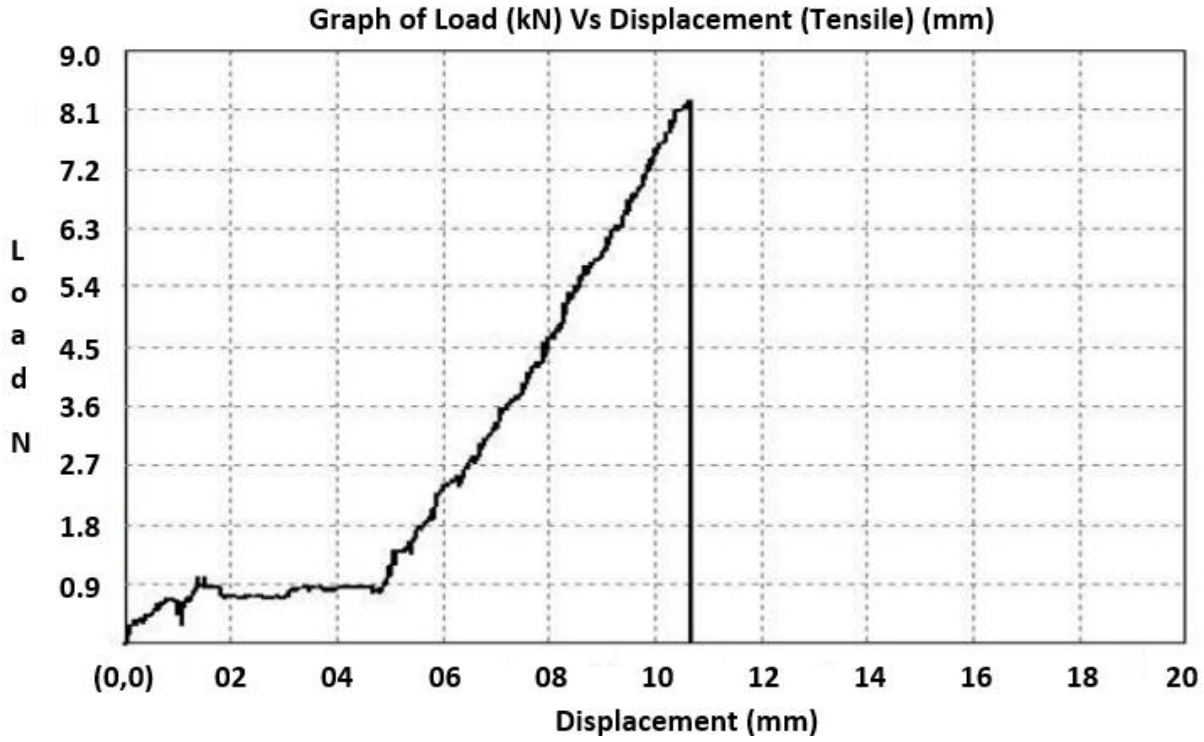

Figure 5.9 Stress-strain characteristics of unmodified CFRP composites

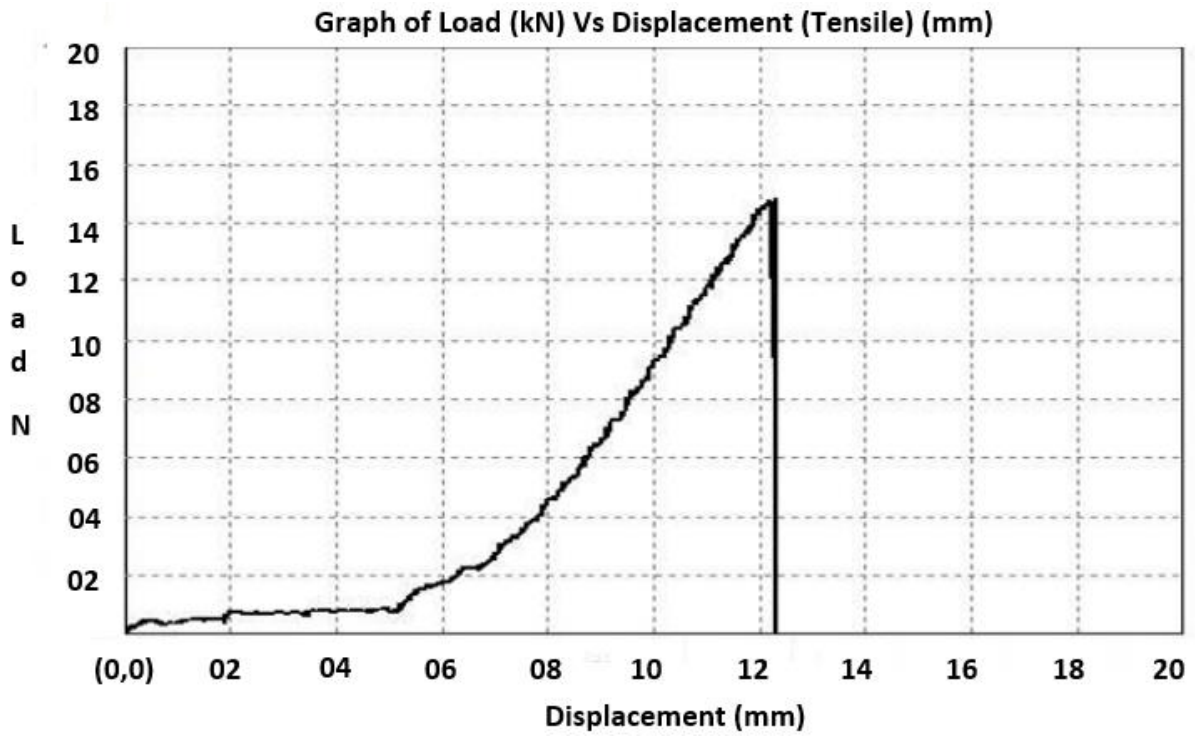

Figure 5.10 Stress-strain characteristics of modified CFRP composites

The DGEBA composite's increased elongation at the break following the 90/10 modification demonstrates that it has less brittle characteristics than unmodified CFRP composites. Additionally, after altering DGEBA with 90/10, the ultimate tensile stress rises from 8.24 kN to 14.84 kN (an increase of 80.1%).

5.5 MODE I ANALYSIS

Mode I (crack opening) loading conditions are adopted as a basic test to evaluate the composite's fiber/matrix adhesion characteristics. One of the most prevalent specimen geometries used to determine the critical energy release rate G_{IC} was the double cantilever beam (DCB) type design (shown in figure 5.11). The Mode I interlaminar toughness was studied using the Double Cantilever Beam (DCB) test carried out to study Interlaminar shear strength (ILSS) and Strain energy release rate (SERR).

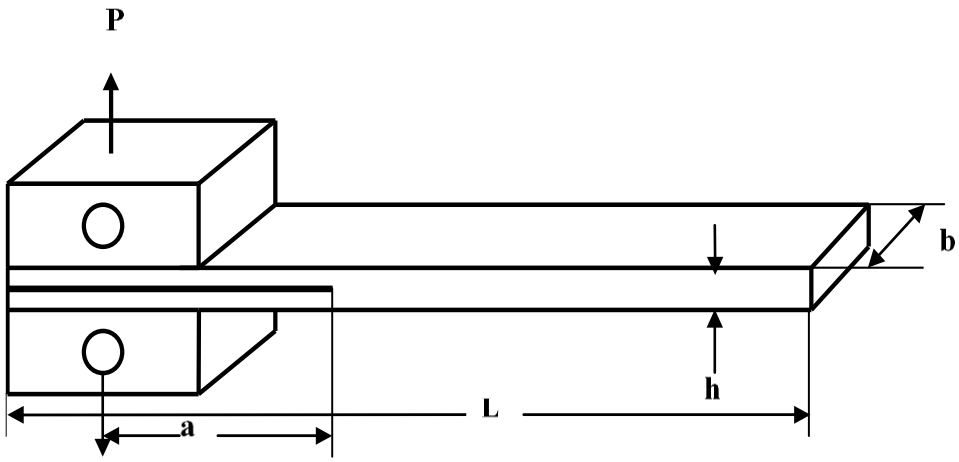

Figure 5.11 Double cantilever beam specimen with load blocks used for Mode I testing

5.5.1 Unmodified CFRP composite

5.5.1.1 Strain energy release rate (SERR)

Using the Modified Beam Theory (MBT) Method, the strain energy release rate (SERR) is determined as follows::

$$G_{IC} = \frac{3P\delta}{2b(a+\Delta)}$$

Specimen width, b = 24.41 mm

Specimen thickness, d = 1.44 mm

Cross-sectional area, A = 35.15 mm^2

Ultimate Tensile Load, P = 30 N

Delamination length, a = 10 mm

Load point displacement, δ = 25.25 mm

$C = \delta/\mathrm{P},\ and\ \Delta = C^{\frac{1}{3}} = 0.94416$

$$G_{IC} = \frac{3 \times 30 \times 25.25}{2 \times 24.41 \times (10 + 0.94416)}$$

$$= 4.253\ N/mm$$

5.5.1.2 Interlaminar shear strength (ILSS)

The Interlaminar shear strength (ILSS) is calculated as follows:

$$ILSS = \frac{0.75P}{bd}$$

$$= \frac{0.75 \times 30}{24.41 \times 1.44}$$

$$= 0.6401 \text{ MPa}$$

The load Vs Displacement graph and Specimen after the DCB test of unmodified CFRP composite as depicted by Figures 5.12 and 5.13 respectively.

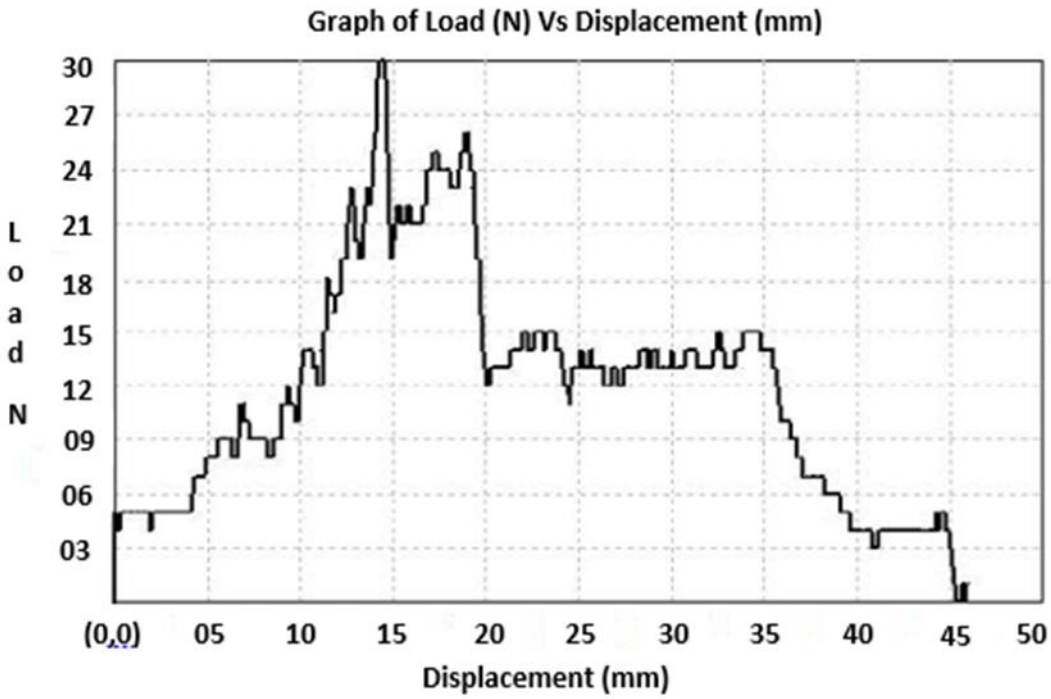

Figure 5.12 Load Vs Displacement graph of Unmodified CFRP composite

Figure 5.13 Unmodified CFRP composite after Mode I Test

5.5.2 Modified 90/10 CFRP composite

5.5.2.1 Strain energy release rate (SERR)

$$G_{IC} = \frac{3P\delta}{2b(a+\Delta)}$$

Specimen width, b = 22.33 mm

Specimen thickness, d = 1.37 mm

Cross-sectional area, A = 30.51 mm^2

Ultimate Tensile Load, P = 48.10 N

Delamination length, a = 10 mm

Load point displacement, δ = 46 mm

$C = \delta/\mathrm{P},\ and\ \Delta = C^{\frac{1}{3}} = 0.98523$

$$G_{IC} = \frac{3 \times 48.10 \times 46}{2 \times 22.33 \times (10 + 0.98523)}$$

$$= 13.53 \text{ N/mm}$$

5.5.2.2 Interlaminar shear strength (ILSS)

$$ILSS = \frac{0.75P}{bd}$$

Specimen width, b = 22.33 mm

Specimen thickness, d = 1.37 mm

Ultimate Tensile Load, P = 48.10 N

$$ILSS = \frac{0.75 \times 48.10}{22.33 \times 1.37}$$

$$= 1.179 \text{ MPa}$$

The load Vs Displacement graph and Specimen after the DCB test of unmodified CFRP composite as depicted by Figures 5.14 and 5.15 respectively.

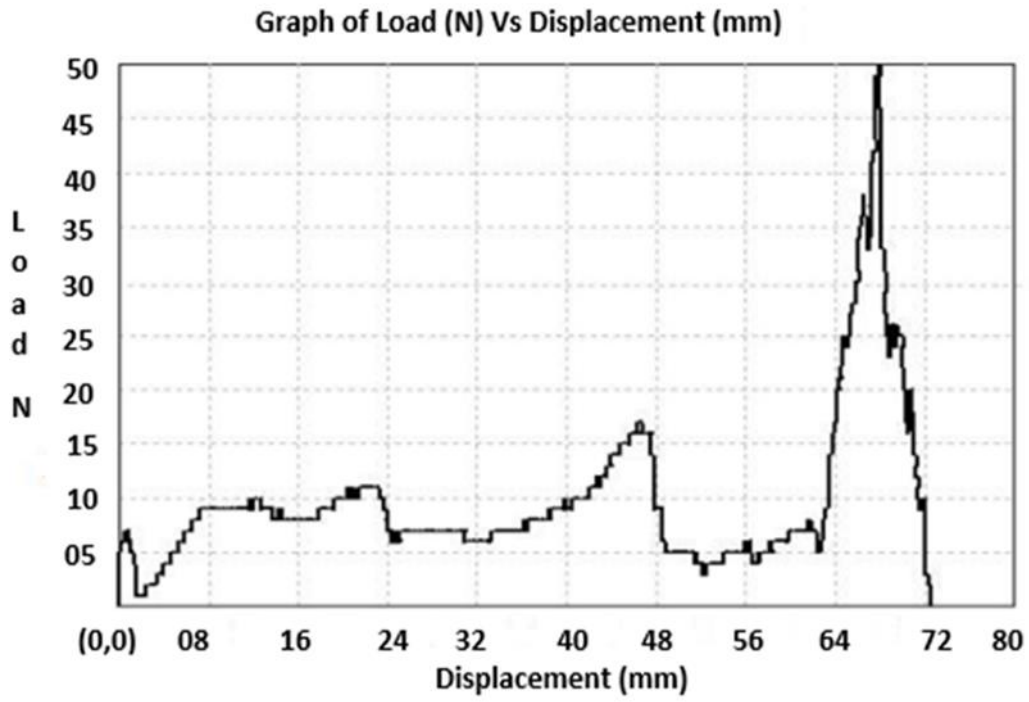

Figure 5.14 Load Vs Displacement graph of Modified 90/10 CFRP composite

Figure 5.15 Modified 90/10 CFRP composite after Mode 1 Test

After Mode I analysis, comparing 90/10 modified CFRP composite specimens to unmodified CFRP composite specimens, average values for interlaminar shear strength (ILSS) and strain energy release rate (SERR) show increases of 84.1% (0.64 to 1.18MPa) and 218.1% (4.25 to 13.53 N/mm), respectively. The enhancement in ILSS and SERR values proves that using PC/ABS blends in DGEBA results in stronger CF laminate adhesives than when using neat epoxy CF laminates.

5.6 MODE II ANALYSIS

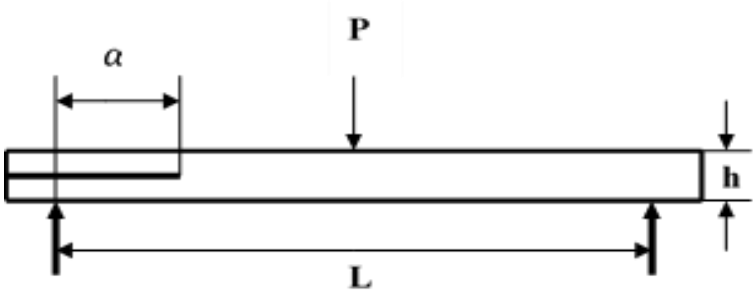

Figure 5.16 Schematic illustration of the end-notched flexure (ENF) specimen for mode-II testing

The end-notched flexure (ENF) test is one of several ways to determine interlaminar fracture toughness in the in-plane shear deformation mode, also known as mode II (Figure 5.16). Mode II analysis was carried out to study Interlaminar shear strength (ILSS) and Strain energy release rate (SERR).

5.6.1 Unmodified CFRP composite

5.6.1.1 Strain energy release rate (SERR)

The strain energy release rate (SERR) is calculated as follows:

$$G_{IIc} = \frac{9P\delta\alpha^2}{2B(\frac{1}{4}L^3 + 3\alpha^3)}$$

Where,

Specimen width, B = 23.42 mm

Specimen thickness, d = 1.44 mm

Cross-sectional area, A = 33.62 mm^2

Ultimate Tensile Load, P = 80.78 N

Delamination length, α = 10 mm

Load point displacement, δ = 7.63 mm

Support span, L = 75 mm

$$G_{IIc} = \frac{9 \times 80.78 \times 7.63 \times 10^2}{2 \times 23.42 \times (\frac{1}{4}(75)^3 + 3 \times (10)^3} = 0.1092 \text{ N/mm}$$

5.6.1.2 Interlaminar shear strength (ILSS)

$$ILSS = \frac{0.75P}{bd}$$

Specimen width, b = 23.42 mm

Specimen thickness, d = 1.44 mm

Ultimate Tensile Load, P = 80.78 N

$$ILSS = \frac{0.75 \times 80.78}{23.42 \times 1.44}$$

$$= 1.179 \text{ MPa}$$

The load Vs Displacement graph and Specimen after the ENF test of unmodified CFRP composite as illustrated in Figures 5.17 and 5.18 respectively.

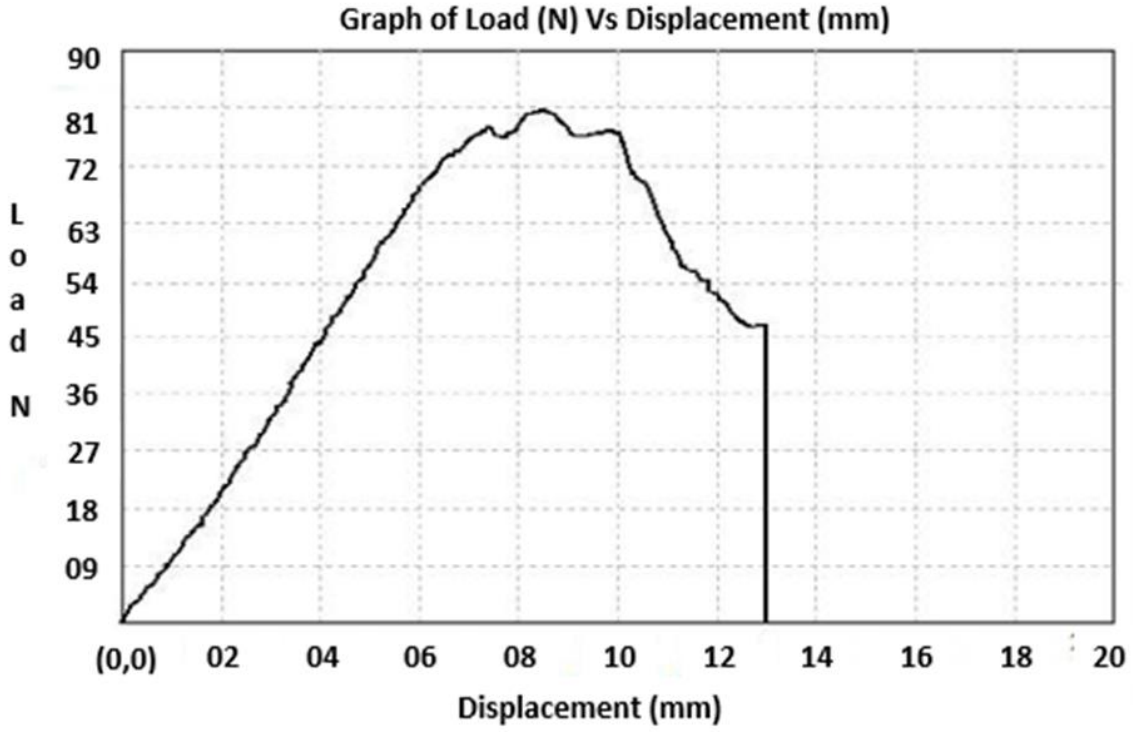

Figure 5.17 Load Vs Displacement graph of Unmodified CFRP composite

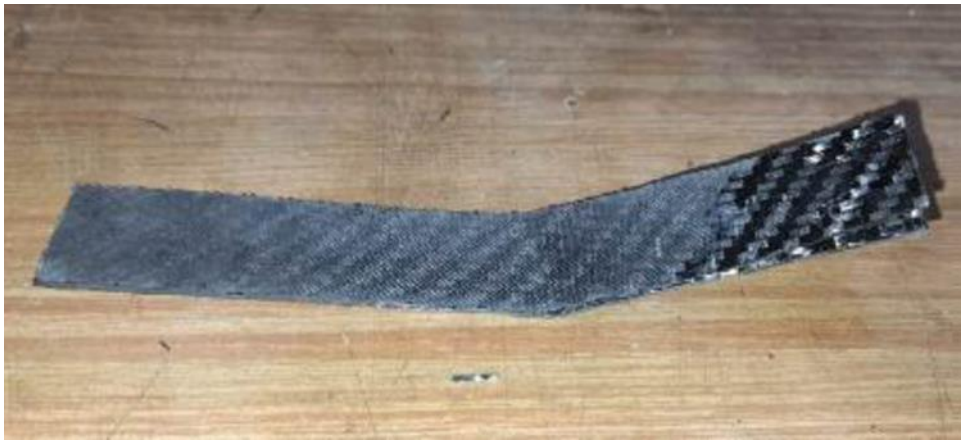

Figure 5.18 Unmodified CFRP composite after Mode II Test

5.6.2 Modified 90/10 CFRP composite

5.6.2.1 Strain energy release rate (SERR)

The strain energy release rate (SERR) is calculated as follows:

$$G_{IIC} = \frac{9P\delta\alpha^2}{2B(\frac{1}{4}L^3 + 3\alpha^3)}$$

Where,

Specimen width, B = 22.07 mm

Specimen thickness, d = 1.41 mm

Cross-sectional area, A = 31.10 mm^2

Ultimate Tensile Load, P = 128.28 N

Delamination length, α = 10 mm

Load point displacement, δ = 9.2 mm

Support span, L = 75 mm

$$G_{IIC} = \frac{9 \times 128.28 \times 9.2 \times 10^2}{2 \times 22.07 \times (\frac{1}{4} \times (75)^3 + 3 \times (10)^3)}$$

$$= 0.2218 \text{ N/mm}$$

5.6.2.2 Interlaminar shear strength (ILSS)

$$ILSS = \frac{0.75P}{bd}$$

Specimen width, b = 22.07 mm

Specimen thickness, d = 1.41 mm

Ultimate Tensile Load, P = 128.28 N

$$ILSS = \frac{0.75 \times 128.28}{22.07 \times 1.41}$$

$$= 3.091 \text{ MPa}$$

The load Vs Displacement graph and Specimen after the ENF test of the Modified 90/10 CFRP composite as shown in Figures 5.19 and 5.20 respectively.

The average values for interlaminar shear strength (ILSS) and strain energy release rate (SERR) after Mode II analysis for 90/10 modified CFRP were compared with unmodified CFRP composite specimens, and an increase of 72.1% (1.79 to 3.09 MPa) and 103.1% (0.109 to 0.22 N/mm) in values are observed respectively. The enhancement in ILSS and SERR values confirms that the presence of PC/ABS blends in DGEBA results in higher adhesive strength with CF laminates than with the case of neat epoxy CF laminates.

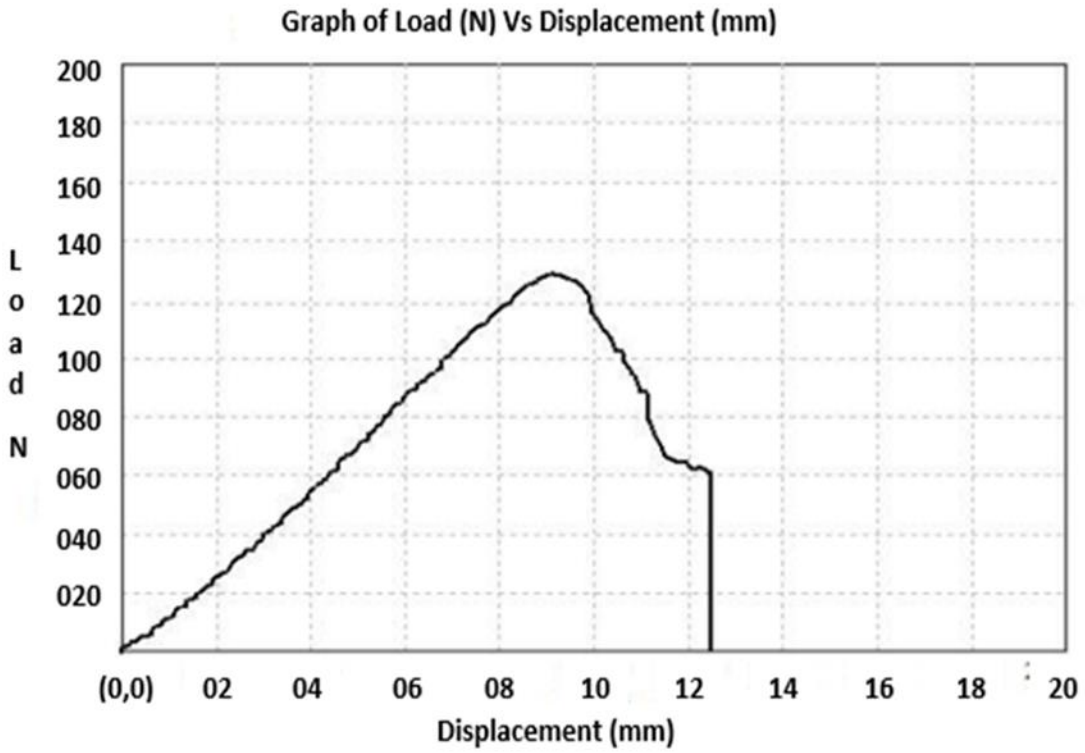

Figure 5.19 Load Vs Displacement graph of Modified 90/10 CFRP composite

Figure 5.20 Modified 90/10 CFRP composite after Mode II Test

5.7 MIX-MODE ANALYSIS

Mix-mode analyses are distinguished by the ratio GI/GII that is driving the crack. The Mixed-Mode Bending (MMB) test integrates the mode I DCB and mode II ENF tests into a single test.

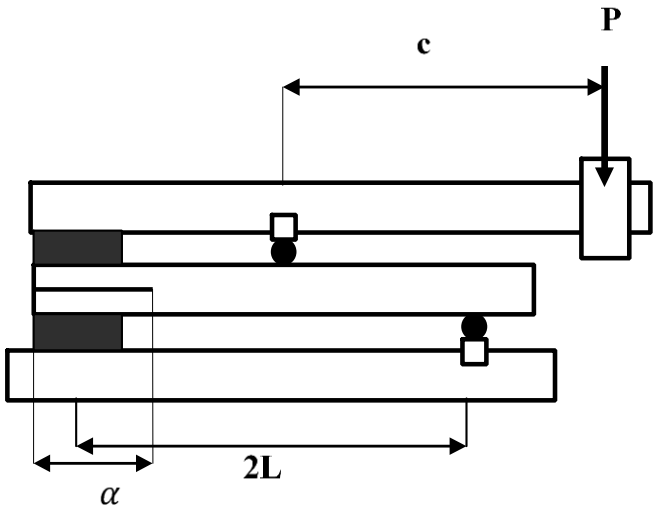

Figure 5.21 Mixed mode I+II interlaminar fracture toughness testing

5.7.1 Unmodified CFRP composite

5.7.1.1 Strain energy release rate (SERR)

$$G_{IIC} = G_{IC} + G_{IIC}$$

$$= 4.645 + 0.01$$

$$= 4.655 \text{ N/mm}$$

5.7.1.2 Interlaminar shear strength (ILSS)

$$ILSS = \frac{0.75P}{bd} = 1.796\ MPa$$

The load Vs Displacement graph and Specimen after the Mix-mode test of Unmodified CFRP composite as shown in Figures 5.22 and 5.23 respectively.

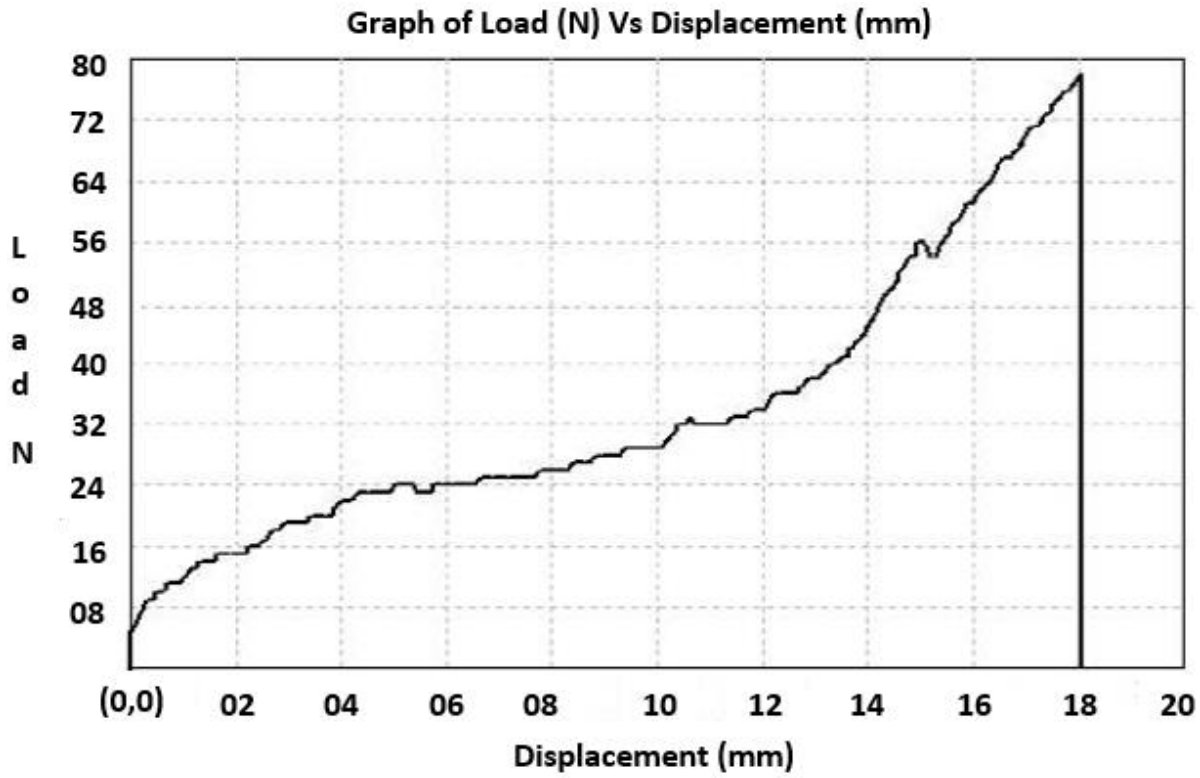

Figure 5.22 Load Vs Displacement graph of Unmodified CFRP composite

Figure 5.23 Unmodified CFRP composite after Mix-mode Test

5.7.2 Modified 90/10 CFRP composite

5.7.2.1 Strain energy release rate (SERR)

$$G_{IIIC} = G_{IC} + G_{IIC}$$

$$= 13.74 + 0.031$$

$$= 13.77 \text{ N/mm}$$

5.7.2.2 Interlaminar shear strength (ILSS)

$$ILSS = \frac{0.75P}{bd} = 3.403\ MPa$$

The load Vs Displacement graph and Specimen after the Mix-mode test of Modified 90/10 CFRP composite as shown in Figures 5.24 and 5.25 respectively.

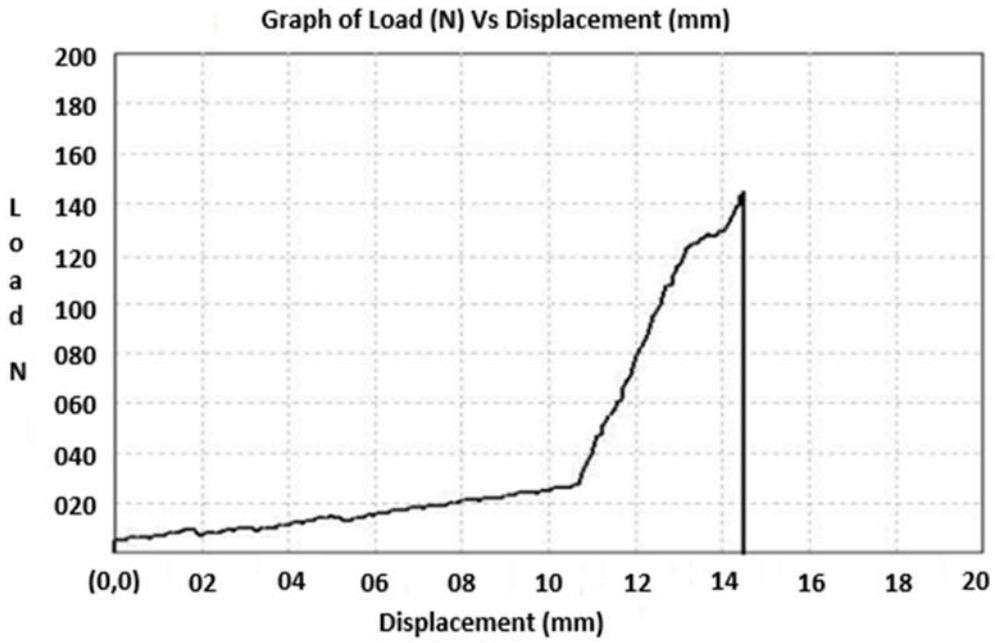

Figure 5.24 Load Vs Displacement graph of Modified 90/10 CFRP composite

Figure 5.25 Modified 90/10 CFRP composite after Mix-mode Test

The average values for interlaminar shear strength (ILSS) and strain energy release rate (SERR) after Mix-mode analysis for 90/10 modified CFRP were compared with unmodified CFRP composite specimens, and an increase of 89.4 % (1.79 to 3.403 MPa) and 195.8 % (4.66 to 13.77 N/mm) in values are observed respectively. The improvement in ILSS and SERR values proves that using PC/ABS blends in DGEBA results in stronger CF laminate adhesives than when using neat epoxy CF laminates.

5.8 SCANNING ELECTRON MICROSCOPY (SEM)

For a better understanding of the synergism resulting from the 90/10 modification of DGEBA epoxy, mode I failure analysis is carried out on the 90/10 modified CFRP composites and compared with unmodified CFRP composites. The same is corroborated using SEM micrographs as shown in figures 5.26 to 5.29. It is clear from comparing figures 5.26 and 5.28 that unmodified CFRP exhibits greater delamination and crack propagation, while 90/10 modified CFRP exhibits less crack density than unmodified CFRP at RT.

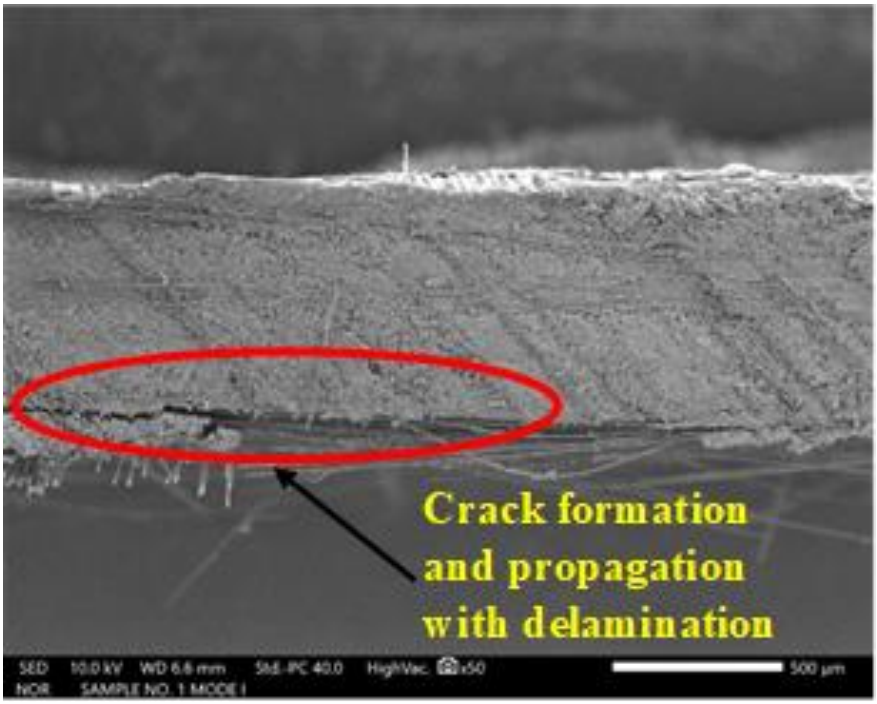

Figure 5.26 SEM image of fracture surface at x50 magnification for unmodified CFRP

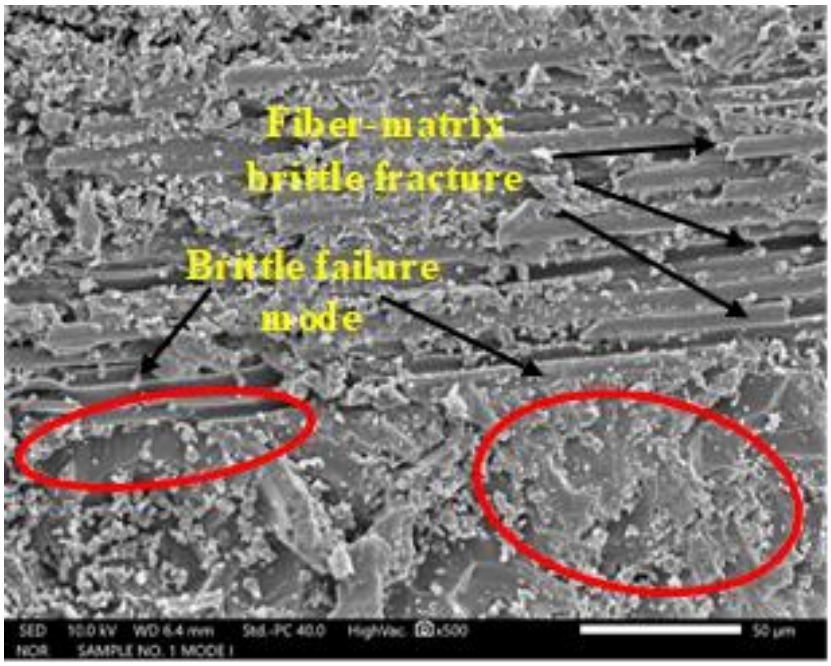

Figure 5.27 SEM image of brittle nature of failure exhibited by unmodified CFRP at x500 magnification

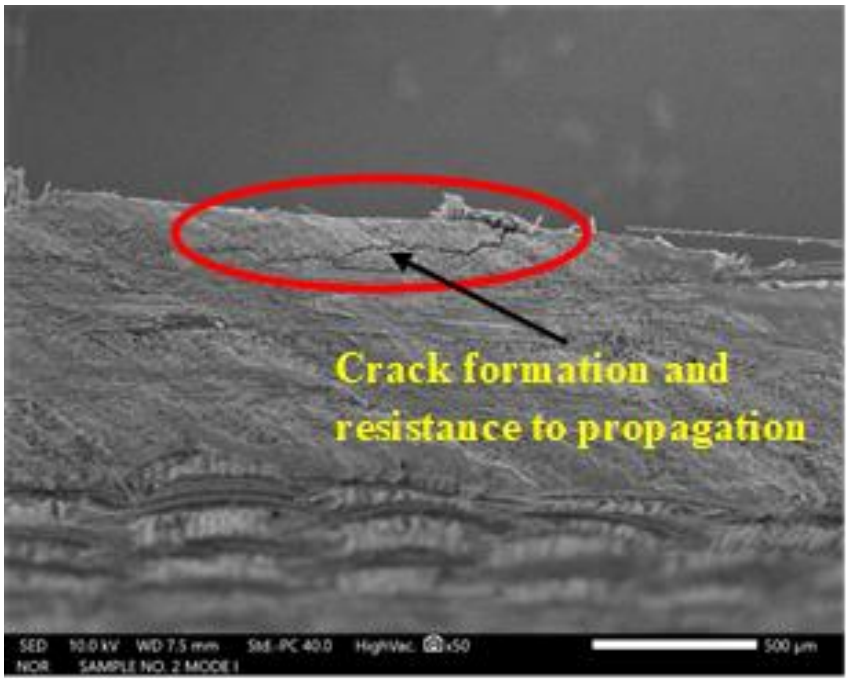

Figure 5.28 SEM image of the fracture surface of 90/10 modified CFRP at x50 magnification

Figure 5.26 SEM image of Nano web-like structure exhibited by 90/10 modified CFRP at x1000 magnification.

It's also noteworthy that the unmodified CFRP exhibits a brittle mode of failure even under RT conditions, with clear instances of delamination and fiber-matrix interface failure confirming weak adhesion of matrix material with CF. When 90/10 modified CFRP composites are used, the CF-matrix interface develops a Nano web-like morphology, which enhances the fracture toughness of the modified CFRP composites and improves their adherence to CF. Additionally, the prominent fiber-matrix failure zones show a large amount of imparted roughness in the fracture characteristics, supporting the ductile failure of the composites during Mode I fracture analysis.

CHAPTER 6

CONCLUSION

In this work, the effect of PC/ABS blend on DGEBA matrix toughening is analyzed at room temperature. Through melt-mixing at 200°C, the PC/ABS with 10% ABS concentration has been shown to be effective in modifying DGEBA epoxy. The synergism effect exhibited by 90/10 blend in modified CFRP composites resulted in improved adhesion and enhanced fracture toughness of CFRP at RT with a great increment in SERR values and a 17.3% increase in elongation at break. By using mode I, mode II and mix mode analysis it is confirmed that the blend 90/10 successful improves the interlaminar strength (ILSS) by 84.2%, 72.1%, and 89.4% respectively and enhances the strain energy release rate (SERR) by 218.1%, 103.1%, and 195.8% respectively. These features support DGEBA's 90/10 modification of its plastic nature, which has greater adhesive strength due to the formation of a nanoweb-like morphology at the fiber-matrix interface. While DGEBA is modified by 90/10, it undergoes a complete curing reaction, same as with DGEBA epoxy that has not been modified when fabricating CFRP composite laminates. Using DSC, it was determined that the 90/10 blend in modified DGEBA worked synergistically to improve thermal stability and increase bond strength (36.3%) between molecules. These properties confirms that the ideal ABS concentration in PC/ABS blends that may be used to modify DGEBA epoxy for upcoming projects or works in the development of structural parts, passenger compartments, and body panels in the automotive sector with superior interlaminar strength and reduced brittle nature.

REFERENCES

1. **Cevdet Kaynak et al.** (2005) Matrix and interface modification of short carbon fiber-reinforced epoxy, *Polymer Testing* 24,455–462
2. **P.F. Liu et al.** (2011) A study on the failure mechanisms of carbon fiber/epoxy composite laminatesusing acoustic emission, *Materials and Design* 37, 228–235,
3. **Muhammad Akhsin Muflikhun et al.** (2020) The evaluation of failure mode behavior of CFRP/Adhesive/SPCC hybrid thin laminates under axial and flexural loading for structural applications, *Composites Part B* 185, 107747
4. **Geng Han et al.** (2016) Failure analysis of carbon fiber reinforced composite subjected to low velocity impact and compression after impact, *Journal of Reinforced Plastics and Composites*,0(0)
5. **Jong H Eun et al.** (2021) Effect of toughened polyamide-coated carbon fiber fabric on the mechanical performance and fracture toughness of CFRP, *Journal of Composite Materials,* 0(0)
6. **K Natarajan et al.** (1994) Toughening studies on an ABS/PC blend-modified epoxy resin system, *High perform.polym*. 6, 241-248
7. **Andrzejewski J, Mohanty AK, Misra M.** (2020) Development of hybrid composites reinforced with biocarbon/carbon fiber system. The comparative study for PC, ABS and PC/ABS based materials. *Compos Part B Eng*, 200: 108319
8. **Ruifeng Liang** and **Rakesh K. Gupta** (2002) SPE 60th ANTEC San Francisco, California, *Vol.3*, *pp*.2948-2952
9. **Abhishek K et al.** (2016) Improved mechanical properties of carbon fiber/graphene oxide-epoxy hybrid composites, *Composites Science and Technology*

10. **Prashanth Turla ety al.** (2014) Interlaminar Shear Strength of Carbon Fiber and Glass Fiber Reinforced Epoxy Matrix Hybrid Composite, *IJREAT International Journal of Research in Engineering & Advanced Technology, Volume 2,* Issue 2

11. **K. Vijaya Kumar et al.** (2017) Experimental Characterization of ILSS of CFRP Laminates, *International Journal of Engineering Research & Technology (IJERT)* ISSN: 2278-0181

12. **Binhua Wang, Nan Dong** and **Guangzhi Ding** (2020) Mode I interlaminar fracture toughness of CFRP laminates reinforced with short aramid fibers, *Journal of Adhesion Science and Technology*

13. M.V. Gordić et al. (2007) Delamination Strain Energy Release Rate in Carbon Fiber/Epoxy Resin Composites, *Materials Science Forum Vol. 555 pp.* 515-519

14. M.S. Sham Prasad et al. (2011) Experimental Methods of Determining Fracture Toughness of Fiber Reinforced Polymer Composites under Various Loading Conditions, *Journal of Minerals & Materials Characterization & Engineering, Vol. 10, No.13, pp.*1263-1275

15. **Hossein Saidpour et al.** (2003) Mode-II Interlaminar Fracture Toughness of Carbon/Epoxy Laminates, *Iranian Polymer Journal 12 (5),* 389-400

16. Yu-xin He et al. (2013) Micro-crack behavior of carbon fiber reinforced thermoplastic modified epoxy composites for cryogenic applications, *Composites: Part B* 44, 533–539

17. Jyotishkumar P et al. (2011) Studies on Stress Relaxation and Thermomechanical Properties of Poly(acrylonitrile-butadiene-styrene) Modified Epoxy-Amine Systems, *Ind. Eng. Chem. Res,* 50, 4432–4440

18. Yongsung Eom et al. (1972) dynamics of void formation upon Curing of epoxy resin

19. **Xiaole Cheng** and **Jeffrey S. Wiggins** (2017) Novel Techniques for the Preparation of Different Epoxy/Thermoplastic Blends, *Springer International Publishing AG 2017 J. Parameswaranpillai et al. (eds.), Handbook of Epoxy Blends*

20. **S. Deng, L. Djukic, R. Paton,** and **L. Ye** (2015) Thermoplastic–epoxy interactions and their potential applications in joining composite structures – A review, *Compos. Part Appl. Sci. Manuf., vol. 68, pp.* 121–132

21. **B. D. Harper, G. H. Staab,** and **R. S. Chen**, (1987) A Note on the Effects of Voids upon the Hygral and Mechanical Properties of AS4/3502 Graphite/Epoxy, *J. Compos. Mater., vol. 21, no. 3, pp.* 280–289

LIST OF PUBLICATIONS

1. **Aravind J, K E Reby Roy, Kasthoori M S** and **Kasthoori Nath A J** (2022) Enhancement of fracture toughness and reduced brittle characteristics of modified CFRP composites by incorporating synergism effect between PC/ABS blend with DGEBA resin systems, *Polymer-Plastics Technology and Materials*,
   DOI: 10.1080/25740881.2022.2084414
2. **Aravind J et al.** (2022) Numerical Analysis to optimise the Effective Thermal resistance of novel waste plastic/SiO2 composite roofing tiles for Residential buildings, *SSRN*